PHYSICAL REVIEW D **76,** 125020 (2007)

Maximally supersymmetric planar Yang-Mills amplitudes at five loops

Z. Bern, J. J. M. Carrasco, and H. Johansson
Department of Physics and Astronomy, UCLA, Los Angeles, California 90095-1547, USA

D. A. Kosower
Service de Physique Théorique, CEA–Saclay, F-91191 Gif-sur-Yvette cedex, France
and Institut für Theoretische Physik, Universität Zürich, CH-8057 Zürich, Switzerland
(Received 7 July 2007; published 19 December 2007)

We present an *Ansatz* for the planar five-loop four-point amplitude in maximally supersymmetric Yang-Mills theory in terms of loop integrals. This *Ansatz* exploits the recently observed correspondence between integrals with simple conformal properties and those found in the four-point amplitudes of the theory through four loops. We explain how to identify all such integrals systematically. We make use of generalized unitarity in both four and D dimensions to determine the coefficients of each of these integrals in the amplitude. Maximal cuts, in which we cut all propagators of a given integral, are an especially effective means for determining these coefficients. The set of integrals and coefficients determined here will be useful for computing the five-loop cusp anomalous dimension of the theory which is of interest for nontrivial checks of the AdS/CFT duality conjecture. It will also be useful for checking a conjecture that the amplitudes have an iterative structure allowing for their all-loop resummation, whose link to a recent string-side computation by Alday and Maldacena opens a new venue for quantitative AdS/CFT comparisons.

DOI: 10.1103/PhysRevD.76.125020 PACS numbers: 11.15.Bt, 11.25.Tq, 11.30.Pb, 11.55.Bq

I. INTRODUCTION

Maximally supersymmetric Yang-Mills theory (MSYM) is an important arena for exploring the properties of gauge theories. The Maldacena weak-strong duality [1] between MSYM and string theory in $AdS_5 \times S^5$ provides an explicit realization of 't Hooft's old dream [2] of expressing the strongly coupled limit of a gauge theory in terms of a string theory. In addition, the higher-loop planar space-time scattering amplitudes of MSYM appear to have a remarkably simple and novel iterative structure [3,4]. This structure allows higher-loop amplitudes to be expressed in terms of lower-loop amplitudes. This simplicity may well be connected to the observed integrability of the theory in the planar limit [5–7].

The iterative structure of the planar amplitudes was first proposed in Ref. [3], and confirmed for the two-loop four-point amplitude. An independent two-loop check was given in Ref. [8]. In Ref. [4], this proposal was fleshed out for all planar maximally helicity violating (MHV) amplitudes, expressed via a specific all-loop exponentiation formula which was confirmed for three-loop four-point amplitudes. The iteration formula has also been shown to hold for two-loop five-point amplitudes [9]. At four loops the amplitudes are known in terms of a set of integrals, but the integrals themselves have not yet been evaluated fully [10,11]. In this paper, we provide the corresponding integral representation of the five-loop four-point planar amplitude, for use in future studies of its properties. In a very recent paper, Alday and Maldacena [12] have shown how to perform a string-side computation of the same gluon amplitudes in the strong-coupling limit. This opens new and exciting possibilities of quantitative checks of the AdS/CFT correspondence, going beyond anomalous dimensions to detailed dependence on kinematics.

In addition to exhibiting an iterative structure, the scattering amplitudes provide new and nontrivial information on the AdS/CFT correspondence. Using considerations of integrability, an integral equation for the cusp (soft) anomalous dimension—valid to all loop orders—was written down by Eden and Staudacher [6]. This equation agreed with the first three loop orders [4,13], but its reliance on various assumptions cast doubt on whether it would hold beyond this. We now know that this original proposal requires modification because of the recent calculation of the four-loop cusp anomalous dimension from the infrared singular terms of a four-loop MSYM amplitude [10,11]. A remarkable new integral equation proposed by Beisert, Eden, and Staudacher (BES) [7] is in agreement with this calculation. Surprisingly, the first four loop orders of the planar cusp anomalous dimension contain sufficient information to test the AdS/CFT correspondence to the level of a few percent [10], using the interpolating function technique introduced by Kotikov, Lipatov, and Velizhanin [14] as well as Padé approximants. This provides an independent guess of the entire perturbative series [10], matching the one generated by the BES integral equation. Detailed studies of the BES equation [15] (see also ref. [16]) confirm that it has the proper behavior [17] at strong coupling, giving a high degree of confidence in it. Nonetheless, further checks on the perturbative side would be quite valuable. The first such check requires a computation of the five-loop anomalous dimension, which—following the approach taken at four loops—requires an expression for the five-loop four-point amplitude.

The unitarity method [18–23] provides a powerful method for computing gauge and gravity loop amplitudes and has played a central role in obtaining MSYM loop amplitudes [3,4,9,10,18,19,24–26]. An important recent improvement [27] is the use of complex momenta [28] within the framework of generalized unitarity [23]. In particular, this allows one to define a nonzero massless three-point amplitude, which vanishes for real momenta. At one loop this enables an easy algebraic determination of the coefficient of any box integral appearing in the theory, because the cut conditions freeze the loop integrals [27]. Some of these ideas have also been applied at two loops [29]. In this paper we apply these ideas to develop a *maximal-cutting* method for efficiently determining coefficients of higher-loop integrals.

In the MSYM theory, a special set of cuts—the iterated two-particle cuts—give rise to the ''rung rule'' for systematically obtaining higher-loop integral representations of planar four-point amplitudes [24,25]. At two and three loops this rule generates all contributions appearing in the amplitudes. However, starting at four loops, new integrals arise which are not generated by the rung rule. In Ref. [10], these were computed explicitly using generalized unitarity by relying on a set of mild assumptions.

These integrals, along with two others that do not appear in the amplitude, are predicted by a procedure relying on a beautiful observation due to Drummond, Henn, Smirnov, and Sokatchev (DHSS) [30]. These authors noticed that, through three loops, the massless integrals appearing in the planar four-point amplitude are in direct correspondence with conformally invariant integrals. This correspondence comes from replacing dimensional regularization with an off shell infrared regularization in four dimensions. We shall call the dimensional regularized version of the conformal integrals *pseudoconformal*, since dimensional regularization breaks conformal invariance. We emphasize that the dual conformal invariance acts in momentum space, and is distinct from the usual conformal invariance of the theory. Its origin and interpretation are still not understood.

DHSS also gave simple rules for generating all such integrals via ''dual diagrams.'' The direct evaluation of generalized unitarity cuts confirmed [10] at four loops that only such pseudoconformal integrals appear in the planar amplitude. In the present work, we will assume that this is also true at higher loops, beginning with five loops. This provides a basis set of integrals for the planar (leading-color) contributions to the five-loop amplitude. We then use the unitarity method to determine the coefficients of these integrals in the planar five-loop four-point amplitude as well as to provide consistency checks on the absence of other integrals.

We make use of an additional observation: the cutting equations hold at the level of the integrands, prior to carrying out any loop integrals. Indeed they hold independently for each of the multiple solutions of the cutting equations. These properties are especially powerful when combined with the basis of pseudoconformal integrals. The problem is then reduced to an algebraic problem of determining the coefficient of each integral. Remarkably, it turns out that after dividing by the tree amplitude, the coefficients are pure numbers taking on the values -1, 0, or 1. This property is already known to hold for the four-point amplitude through four loops [10], and here we confirm it through five loops.

At one loop, complete dimensionally regularized amplitudes in the MSYM theory can be constructed using only four-dimensional helicity amplitudes, greatly simplifying their construction [18,19]. Unfortunately, no such theorem exists at higher loops. Any rigorous construction of amplitudes requires that D-dimensional momenta be used in the cuts. It is worth noting that if our assumption of a pseudoconformal basis of integrals is correct, with dimension independent coefficients, then unitarity in four dimensions *does* suffice to determine these amplitudes in all dimensions. Our partial checks of D-dimensional cuts provide nontrivial evidence that this assumption is correct. This is rather remarkable because away from four dimensions there is *a priori* no reason why a simple analytic continuation of the dimension of the integrals should give correct results.

Our expression for the five-loop four-point planar MSYM amplitude in terms of integral functions should be useful in a number of studies. The infrared singularities present in the amplitude encode the so-called cusp or soft anomalous dimension. At five loops these singularities begin at $1/\epsilon^{10}$ [where ϵ, as usual, is the dimensional regularization parameter: $\epsilon = (4 - D)/2$]. Evaluation of the infrared singular terms through $1/\epsilon^2$ would allow the extraction of the five-loop cusp anomalous dimension, as has been done at three and four loops [4,10]. An evaluation though order $1/\epsilon$ would allow the extraction of a second anomalous dimension connected to a form factor. An evaluation through $\mathcal{O}(\epsilon^0)$ would allow a five-loop check of the iterative structure of the amplitudes, providing strong evidence that it continues to all loop orders. Although evaluating loop integrals is rather challenging, there has been rapid progress using Mellin-Barnes representations [31] and in automating the required analytic continuations [32], allowing for explicit computations through four loops. Recently, there has also been progress in isolating the subsets of terms which determine the anomalous dimension [11], greatly simplifying its calculation. Further development will presumably be needed to apply these advances to the five-loop amplitude.

Another important reason for studying MSYM amplitudes is their intimate connection to $\mathcal{N} = 8$ supergravity amplitudes. The identification of additional cancellations in this theory [33] suggests that in four dimensions it may be ultraviolet finite to all loop orders [34,35]. (See also Ref. [36].) String dualities also hint at UV finiteness for

$\mathcal{N} = 8$ supergravity [37], although this is weakened by issues with towers of light nonperturbative states from branes wrapped on the compact dimensions [38]. Remarkably, computational advances for gauge theory amplitudes can be imported [25] directly into calculations of gravity amplitudes, by combining the unitarity method with the Kawai-Lewellen-Tye [39] tree-level relations between gauge and gravity theories. This allows cuts of gravity loop amplitudes to be expressed as double copies of cuts of corresponding gauge theory amplitudes [25]. This strategy has recently been applied to obtain the three-loop four-point amplitude of $\mathcal{N} = 8$ supergravity, starting from corresponding $\mathcal{N} = 4$ MSYM amplitudes [35]. That computation shows that at least through three loops, MSYM and $\mathcal{N} = 8$ supergravity share the same ultraviolet power counting. Because they share the same critical dimension for ultraviolet finiteness, both are ultraviolet finite in four dimensions. The five-loop planar super-Yang-Mill amplitudes obtained here will be an important input for obtaining the corresponding five-loop supergravity amplitudes. (The supergravity calculation also requires the nonplanar contributions.)

The paper is organized as follows. In Sec. II, we briefly summarize known properties of the amplitudes and define the notation used in the remainder of the paper. In Sec. III, we review the observations of Refs. [10,30], on the exclusive appearance of pseudoconformal integrals in planar four-point amplitudes. Because candidate integrals proliferate as the number of loops increases, we give a systematic procedure in Sec. IV for constructing these integrals. The results of this procedure at five loops are given in Sec. V, along with the coefficients of the integrals determined via unitarity. Our *Ansatz* for the amplitude is also presented in this section. We then briefly review generalized unitarity in Sec. VI. A description of the cuts used to determine the integral coefficients is given in Secs. VII and VIII, along with a description of the method of maximal cuts introduced in this paper. Our conclusions and some comments on the outlook are given in Sec. IX.

II. NOTATION AND REVIEW OF MSYM AMPLITUDES

We use a standard color decomposition [21,40] for the MSYM amplitudes in order to disentangle color from kinematics. In this paper we focus on the leading-color planar contributions, which have a color structure similar to those of tree amplitudes, up to overall factors of the number of colors, N_c. The color-decomposed form of planar contributions to the L-loop $SU(N_c)$ gauge-theory n-point amplitudes is

$$\mathcal{A}_n^{(L)} = g^{n-2}\left[\frac{2e^{-\epsilon\gamma}g^2N_c}{(4\pi)^{2-\epsilon}}\right]^L \sum_\rho \mathrm{Tr}(T^{a_{\rho(1)}}T^{a_{\rho(2)}}\cdots T^{a_{\rho(n)}}) \times A_n^{(L)}(\rho(1),\rho(2),\ldots,\rho(n)), \tag{2.1}$$

where $A_n^{(L)}$ is an L-loop color-ordered partial amplitude. We have followed the normalization conventions of Ref. [4]. Here γ is Euler's constant, and the sum runs over noncyclic permutations, ρ, of the external legs. In this expression we have suppressed labels of momenta and helicities, leaving only the indices identifying the external legs. Our convention is that all legs are outgoing. This decomposition holds for all particles in the gauge supermultiplet.

We also define a loop amplitude normalized by the tree amplitude,

$$M_n^{(L)} \equiv A_n^{(L)}/A_n^{\mathrm{tree}}. \tag{2.2}$$

Supersymmetry Ward identities [41] guarantee that, after dividing out by the tree amplitudes, MHV amplitudes are identical for any helicity configuration [22]. (The complete set of these tree amplitudes are tabulated in Appendix E of Ref. [25].) Because four-point amplitudes are always maximally helicity violating, this holds for all four-point amplitudes. Because it is independent of the position of the two negative helicity legs, $M_n^{(L)}$ has complete cyclic and reflection symmetry. A practical consequence of this is that once a coefficient of a given integral is determined, the coefficient of integrals related by cyclic or reflection symmetry follow trivially.

In our evaluations of four-dimensional unitarity cuts, we use the spinor helicity formalism [40,42], in which the amplitudes are expressed in terms of spinor inner products,

$$\begin{aligned} \langle jl\rangle &= \langle j^-|l^+\rangle = \overline{u}_-(k_j)u_+(k_l), \\ [jl] &= \langle j^+|l^-\rangle = \overline{u}_+(k_j)u_-(k_l), \\ \langle a^-|k_b + k_c|d^-\rangle &= \overline{u}_-(k_a)[\not{k}_b + \not{k}_c]u_-(k_d), \end{aligned} \tag{2.3}$$

where $u_\pm(k)$ is a massless Weyl spinor with momentum k and positive or negative chirality. Our conventions follow the QCD literature, with $[ij] = \mathrm{sgn}(k_i^0k_j^0)\langle ji\rangle^*$ for real momenta so that

$$\langle ij\rangle[ji] = 2k_i\cdot k_j = s_{ij}. \tag{2.4}$$

We also define

$$\lambda_{k_i} \equiv u_+(k_i), \qquad \tilde{\lambda}_{k_i} \equiv u_-(k_i). \tag{2.5}$$

For complex momenta these two spinors are independent, though they are dependent for real momenta.

In Ref. [3], a conjecture was presented that MSYM amplitudes possess an iterative structure, based on an observed iteration of two-loop four-point amplitudes. In Ref. [4], this was fleshed out for MHV amplitudes into an explicit exponentiation *Ansatz* to all loop orders. Through five loops, the expansion of the exponential gives the iteration relations,

$$M_n^{(2)}(\epsilon) = \tfrac{1}{2}(M_n^{(1)}(\epsilon))^2 + f^{(2)}(\epsilon)M_n^{(1)}(2\epsilon) + C^{(2)} + \mathcal{O}(\epsilon), \tag{2.6}$$

$$M_n^{(3)}(\epsilon) = -\tfrac{1}{3}[M_n^{(1)}(\epsilon)]^3 + M_n^{(1)}(\epsilon)M_n^{(2)}(\epsilon) + f^{(3)}(\epsilon)M_n^{(1)}(3\epsilon) + C^{(3)} + \mathcal{O}(\epsilon), \tag{2.7}$$

$$M_n^{(4)}(\epsilon) = \tfrac{1}{4}[M_n^{(1)}(\epsilon)]^4 - [M_n^{(1)}(\epsilon)]^2M_n^{(2)}(\epsilon) + M_n^{(1)}(\epsilon)M_n^{(3)}(\epsilon) + \tfrac{1}{2}[M_n^{(2)}(\epsilon)]^2 + f^{(4)}(\epsilon)M_n^{(1)}(4\epsilon) + C^{(4)} + \mathcal{O}(\epsilon), \tag{2.8}$$

$$M_n^{(5)}(\epsilon) = -\tfrac{1}{5}[M_n^{(1)}(\epsilon)]^5 + [M_n^{(1)}(\epsilon)]^3M_n^{(2)}(\epsilon) - [M_n^{(1)}(\epsilon)]^2M_n^{(3)}(\epsilon) - M_n^{(1)}(\epsilon)[M_n^{(2)}(\epsilon)]^2 + M_n^{(1)}(\epsilon)M_n^{(4)}(\epsilon) + M_n^{(2)}(\epsilon)M_n^{(3)}(\epsilon) + f^{(5)}(\epsilon)M_n^{(1)}(5\epsilon) + C^{(5)} + \mathcal{O}(\epsilon), \tag{2.9}$$

where $f^{(L)}(\epsilon)$ is a three term series in ϵ,

$$f^{(L)}(\epsilon) = f_0^{(L)} + \epsilon f_1^{(L)} + \epsilon^2 f_2^{(L)}, \tag{2.10}$$

and $f_i^{(L)}$ are numbers independent of the kinematics and of the number of external legs n. Similarly, the $C^{(L)}$ are also pure numbers. The constant $f_0^{(L)}$ is proportional to the L-loop cusp (soft) anomalous dimension $\gamma_K^{(L)}$,

$$f_0^{(L)} = \tfrac{1}{4}\gamma_K^{(L)}. \tag{2.11}$$

After subtracting the known infrared singularities [43] the iteration relation takes on a rather simple exponential form,

$$\mathcal{F}_n(0) = \exp[\tfrac{1}{4}\gamma_K F_n^{(1)}(0) + C], \tag{2.12}$$

where $F_n^{(1)}(0)$ is the n-point one-loop finite remainder, γ_K is the complete cusp anomalous dimension, and C depends on the coupling but not on the external momenta. Very recently Alday and Maldacena have matched this expression at strong coupling for $n = 4$ using string theory [12].

The iteration conjecture has so far been confirmed for two- and three-loop four-point amplitudes [3,4] as well for two-loop five-point amplitudes [9]. For the four-loop four-point amplitude, the integrand is known [10] and has been shown to generate the correct form of the infrared singularities through $\mathcal{O}(1/\epsilon^2)$. This has been used to extract the four-loop contribution to the cusp anomalous dimension [10,11] numerically.

As the amplitudes are infrared divergent, we need to regulate them. In order to preserve the supersymmetry we use the four-dimensional helicity (FDH) scheme [44], which is a relative of Siegel's dimensional reduction scheme [45].

III. PSEUDOCONFORMAL INTEGRALS

Conformal properties offer a simple way to identify integrals that can appear in planar MSYM amplitudes [10,30]. This observation allows us to easily identify a basis of integrals, whose coefficients can be determined via the unitarity method. This greatly simplifies the cut analysis because we need to determine only these coefficients to obtain the planar amplitudes.

Although the underlying theory is conformally invariant, there is as yet no proof that only integrals dictated by conformal invariance can appear. One obvious complication to providing such a proof is the infrared divergence of the amplitudes, and the subsequent need to regulate the integrals (via dimensional regularization), which breaks the dual conformal invariance. As mentioned in Sec. I, we therefore call the integrals corresponding to conformally invariant ones "pseudoconformal." We shall describe in this section how to implement this correspondence. In principle, it is possible that individual integrals appearing in the amplitude would have no special conformal properties, yet the complete amplitude would retain simple conformal properties because of cancellations between integrals. Through four loops [10], however, only pseudoconformal integrals appear in the four-point amplitude. This provides compelling evidence that this is a general property of MSYM four-point amplitudes.[1]

We therefore assume that only pseudoconformal integrals appear in the five-loop planar amplitudes. One way of proving the correctness of this assumption would be to compute a sufficient number of cuts in D dimensions to determine the amplitude completely. In this paper, we discuss only a partial confirmation.

Dimensional regulation of the infrared singularities breaks the conformal symmetry. For the purposes of exposing the conformal symmetry, we instead regulate the infrared divergences by taking the external momenta k_i off shell and letting the dimension be $D = 4$. We will obtain a pseudoconformal integral from a suitable conformal integral by reversing this change of regulator.

The authors of Ref. [30] provide a simple way of making manifest the conformal properties of planar integrals via "dual diagrams." The dual diagrams provide a direct method of identifying all conformally invariant loop integrals.[2] In general, conformal properties are not obvious in the momentum-space representation of loop integrals, but with a simple change of variables encoded by the dual diagrams we can make these properties manifest.

Let us give an illustrative example. Consider the two-loop double-box integral of Fig. 1(a),

[1]For higher-point amplitudes, the situation is more complicated, as can be confirmed by checking the conformal properties of known results [9] for the five-point amplitudes at two loops.

[2]The dual diagrams are related to the dual graphs used in graph theory [46].

$$I^{(2)}(s,t) = (-ie^{\epsilon\gamma}\pi^{-D/2})^2 s^2 t \int \frac{d^D p d^D q}{p^2(p-k_1)^2(p-k_1-k_2)^2 q^2(q-k_4)^2(q-k_3-k_4)^2(p+q)^2}, \tag{3.1}$$

where $s = (k_1 + k_2)^2$ and $t = (k_2 + k_3)^2$.

After replacing the regulator as mentioned above, the conformal symmetry can then be exposed via the change of variables,

$$k_1 = x_{41}, \qquad k_2 = x_{12}, \qquad k_3 = x_{23}, \qquad k_4 = x_{34}, \qquad p = x_{45}, \qquad q = x_{64}, \tag{3.2}$$

where $x_{ij} \equiv x_i - x_j$. The new variables automatically satisfy momentum conservation

$$x_{41} + x_{12} + x_{23} + x_{34} = 0 \Leftrightarrow k_1 + k_2 + k_3 + k_4 = 0. \tag{3.3}$$

After substituting the new variables into Eq. (3.1) and taking $D = 4$, the double-box integral takes on a very symmetric form,

$$I^{(2)}(s,t) = (-i\pi^{-2})^2 x_{24}^4 x_{13}^2 \int \frac{d^4 x_5 d^4 x_6}{x_{45}^2 x_{15}^2 x_{25}^2 x_{46}^2 x_{36}^2 x_{62}^2 x_{56}^2}. \tag{3.4}$$

The conformal-invariance properties follow from examining its behavior under inversion, $x^\mu \to x^\mu / x^2$,

$$x_{ij}^2 \to \frac{x_{ij}^2}{x_i^2 x_j^2}, \qquad d^4 x_i \to \frac{d^4 x_i}{x_i^8}. \tag{3.5}$$

Under this inversion the double box (3.4) is invariant because each external point x_1, x_2, x_3, x_4 appears equally many times in the numerator as in the denominator, while the internal points x_5, x_6 appear exactly four times in the denominator, precisely canceling the behavior of the integration measure. The x variables are useful because inversion respects momentum conservation, which is not true for an inversion of the original momentum variables.

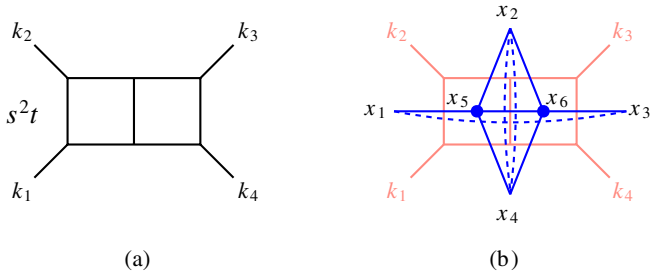

FIG. 1 (color online). The two-loop planar double-box integral (a) and its dual (b) overlaying a faded version of (a). In (b) the dashed lines represent a numerator factor of $(x_{24}^2)^2 x_{13}^2 = s^2 t$. This inserted numerator factor is needed for conformal invariance of the integral.

More generally, following Refs. [10,30], we keep track of conformal weights using dual diagrams. To obtain the dual representation, start with the momentum representation shown in Fig. 1(a) and place internal points x_5, x_6 inside each loop, as well as external points x_1, x_2, x_3, x_4 between each pair of external momenta, as shown in Fig. 1(b). Following Ref. [30] we mark the internal integration points by solid dots at the center of each loop but in most cases leave the external points unmarked. Solid lines represent an inverse power of x_{ij}^2, corresponding to the dual propagator $1/x_{ij}^2$, which crosses exactly one Feynman propagator whose momentum is equal to x_{ij}. Dashed lines represent a positive power of an x_{ij}^2, such as the numerator factors of $s = x_{24}^2$ and $t = x_{13}^2$. The x_{ij}^2 represented by a dashed line correspond the sum of the momenta of the ordinary propagator lines they cross. (The dashed lines can be deformed to cross different propagators, but momentum conservation ensures that this does not affect the value of the dual invariants x_{ij}^2.) The dual diagram constructed in Fig. 1(b) is in direct correspondence to the dual integral (3.4).

We can further restrict the possible set of conformal integrals by requiring that they have only logarithmic behavior in the on shell limit. That is, we are not interested in conformal integrals which vanish or diverge with a power-law behavior in any k_i^2, because these do not correspond to massless integrals in dimensional regularization. For example, numerator factors such as $x_{12}^2 = k_2^2$ are not allowed. Similarly, factors such as $1/x_{12}^2 = 1/k_2^2$ are excluded because their power singularities are too severe for the required logarithmic behavior of infrared singularities. We then obtain a pseudoconformal integral, as discussed earlier, by replacing the off shell regulator with the usual dimensional one.

It is straightforward to generalize this graphical mapping to any loop order, allowing for a relatively simple bookkeeping of the change of variables between the momenta and the dual x_i variables. The map in Eq. (3.2) exemplifies the convention we use for external momenta for all diagrams in this paper.

The conformal weights are easy to read off directly from the dual diagrams. For a dual diagram to be conformally invariant it must satisfy the following: The number of solid lines minus the number of dashed lines entering a point x_i must be zero for external points, and four for internal points. The conformal weight of four for internal points cancels the conformal weight of the integration measure given in Eq. (3.5). As observed in Ref. [10], a consequence of requiring integrals to be conformal is that integrals with triangle or bubble subdiagrams are not allowed.

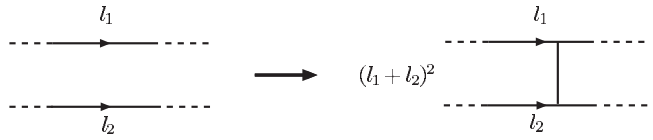

FIG. 2. The rung rule for generating higher-loop integrands from lower-loop ones.

One class of pseudoconformal integrals may be understood in terms of the "rung rule" of Ref. [24]. This rule instructs its user to generate contributions to an $(L + 1)$-loop amplitude from a known L-loop amplitude by inserting a new leg between each possible pair of internal legs, as shown in Fig. 2. From this set, all diagrams with either triangle or bubble subdiagrams are removed. The new loop momentum is integrated over, after including an additional factor of $(l_1 + l_2)^2$ in the numerator, where l_1 and l_2 are the momenta flowing through the indicated lines. (With the conventions used here it is convenient to remove a factor of i from the numerator factor, compared to Ref. [24].) Each distinct contribution should be counted only once, even if it can be generated in multiple ways. Contributions arising from identical diagrams (that is, having identical propagators) but with distinct numerators count as distinct contributions. The diagrams obtained by iterating this procedure are sometimes called Mondrian diagrams, because of their similarity to Mondrian's art.

The rung rule may be understood as a consequence of the conformal properties of the integrals. As illustrated in Fig. 3, if the starting integral is pseudoconformal, inserting a rung splits the inner loop into two side-by-side loops, and the conformal weight of the central dots in the figure is unchanged. However, the upper and lower loop need an additional dashed line connecting their central dots to maintain their conformal weight. This dashed line corresponds exactly to the factor of $(l_1 + l_2)^2$ required by the rung rule in Fig. 2.

The rung rule, unfortunately, does not generate the complete set of planar integrals [10]. However, at least through four loops any diagram that it generates is obtained with the correct sign. Here we confirm this observation at five loops, using the unitarity method. To obtain the remaining, non-rung-rule contributions to the five-loop amplitude, we start with the other pseudoconformal integrals and determine their coefficients using the unitarity method.

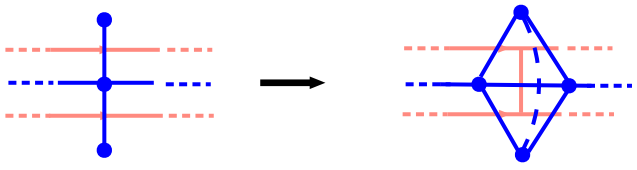

FIG. 3 (color online). The rung rule maintains conformal weight. If the dual diagram prior to applying the rung rule has the proper conformal weight so will the resulting diagram.

IV. GENERATING THE PLANAR PSEUDOCONFORMAL DIAGRAMS

The proliferation of candidate pseudoconformal integrals with increasing number of loops encourages the development of a systematic construction procedure. One approach is suggested by examining the $(L + 1)$-particle cuts of an L-loop amplitude. Using such a cut we can decompose the loop integrals into products of tree diagrams which then simplifies the bookkeeping.[3] Our procedure will be

(1) Construct the set of all possible amputated tree configurations on each side of the cut.
(2) Identify all possible loop integrals by sewing each configuration from the left side of the cut with each configuration on the right side of the cut.
(3) Identify all possible overall factors in each integral which make it conformal.

Because the conformal properties are most obvious in the dual representation described in Sec. III, we have found it convenient to work with dual coordinates and translate back to the momentum representation at the end.

A. Constructing all dual tree diagrams

It is useful to consider first the reverse procedure of splitting an L-loop integral into two trees via an $(L + 1)$-particle cut. As an illustration, consider the four-loop "window" integral as cut in Fig. 4. This integral contributes to the four-loop four-point amplitude [10]. As shown in the figure, a five-particle cut separates the integral into a product of two tree diagrams. In dual space, we also split integrals into tree diagrams with a five-particle cut. Figure 5 depicts the separation of the corresponding dual diagram into tree diagrams, which we carry out in two steps. In the first step of the figure we divide the dual diagram along the cut marked with arrows, keeping the cut line on both sides. In the next step we drop the lines with arrows, giving us dual diagrams corresponding to amputated (i.e., with external propagators removed) tree-level momentum-space diagrams. In this representation each dual line crosses an internal propagator of the momentum-space diagrams. The diagrams will always have a fixed cyclic ordering. The dual-diagram points also respect this cyclic ordering. In this example, for the tree amplitude on the left, the points are ordered $\{x_4, x_1, x_2, x_8, x_7, x_6, x_5\}$, while the points for the tree diagram on the right are ordered $\{x_2, x_3, x_4, x_5, x_6, x_7, x_8\}$.

Our systematic construction of all dual loop diagrams simply reverses the process in this example. At L loops we

[3]At six loops and beyond it turns out that there are pseudoconformal integrals which do not have an $(L + 1)$-particle cut. These can however be obtained from a "parent diagram" containing an $(L + 1)$-particle cut, by canceling one of the propagators.

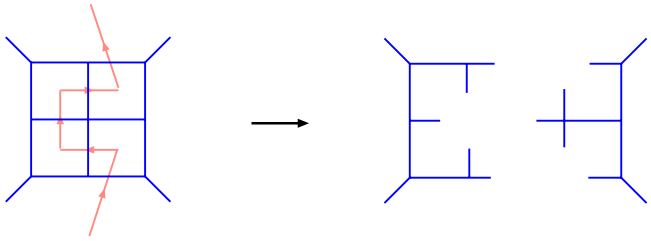

FIG. 4 (color online). The four-loop window diagram. The lighter colored line running through the diagrams is a five-particle cut which separates the diagram into a product of tree diagrams.

start with two ordered lists of $L+3$ points: $\{x_1, x_2, x_{L+4}, x_{L+3}, \ldots, x_5, x_4\}$ for the left tree and $\{x_2, x_3, x_4, x_5, \ldots, x_{L+4}\}$ for the right tree. These lists correspond to $(L+1)$-particle cuts in the s_{12} channel; the corresponding construction in the s_{23} channel is easily obtained by relabeling the final result. The assignment of labels x_1, x_2, x_3, x_4 to points is determined by the external momenta, and the remainder follow from the cyclic ordering.

We obtain all possible pairs of dual tree diagrams by connecting nonadjacent points with $1/x_{ij}^2$ propagators in all possible ways such that the lines do not cross. Dual diagrams where nearest-neighbor points are connected are not included as they correspond to momentum-space diagrams whose external propagators have not been truncated.

After identifying the possible dual tree diagrams we restore the dual lines representing the cut, by retracing our steps in the example shown in Fig. 5. That is, in both sets of tree diagrams we draw lines with arrows connecting x_4 to x_5, etc., to x_{L+4}, which is then connected to x_2. Once this is done the pairs of tree diagrams can be glued together along the lines with arrows, which then gives us the L-loop dual diagrams that we wish to construct. At this stage we can remove diagrams trivially related by cyclic or flip symmetry.

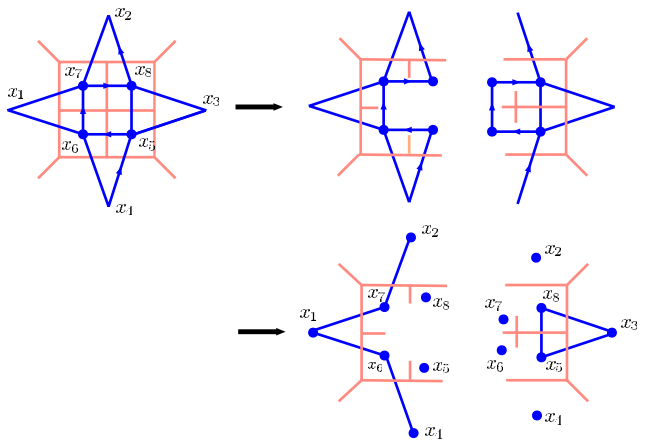

FIG. 5 (color online). The dual diagram corresponding to the window diagram. The lines with the arrows indicate the cut which separates the dual diagram into a product of tree dual diagrams.

B. Finding the pseudoconformal integrals

Once we have a set of candidate loop-level dual diagrams, we must find the numerator factors necessary to make the corresponding integrals conformal. This can be accomplished as follows [10,30]:

(i) If one of the internal points $\{x_5, x_6, \ldots, x_{L+4}\}$ appears in less than four dual propagators, discard the diagram as it cannot be made conformal.

(ii) To determine possible numerator factors one first identifies all external points from the set $\{x_1, x_2, x_3, x_4\}$ appearing in one or more dual propagators, and all internal points in the set $\{x_5, x_6, \ldots, x_{L+4}\}$ appearing in five or more dual propagators. All such points require numerator factors x_{ij}^2 to cancel the extra conformal weight. That is, the number of times a given external x_i appears in the dual propagators minus the number of times it appears in the numerator should be zero. Similarly, for an internal point x_i, the number of times it appears in the dual propagators minus the number of times it appears in the numerator should be four. To find the conformally invariant integrals we sweep through products of all candidate numerators x_{ij}^2 to identify the ones where the conformal-invariance constraints are satisfied. (In principle, there might also be an overall resulting factor of $1/s = 1/x_{24}^2$ or $1/t = 1/x_{13}^2$, but this does not occur at five loops, nor do we expect such contributions to enter the amplitudes with nonzero coefficients at any loop order.)

(iii) If the previous step yields a previously identified pseudoconformal integral, go on to the next case. Such repeated integrals can arise when a numerator factor cancels a propagator or when diagrams are related by symmetries.

Once we have the set of conformal dual diagrams we can convert these back to momentum space with a change of variables,

$$\begin{aligned} &k_1 = x_{41}, \quad k_2 = x_{12}, \quad k_3 = x_{23}, \quad k_4 = x_{34}, \\ &l_1 = x_{45}, \quad l_2 = x_{56}, \quad \ldots, \quad l_{L+1} = x_{(L+4)2}, \end{aligned} \tag{4.1}$$

where the l_i are the momenta of the lines in

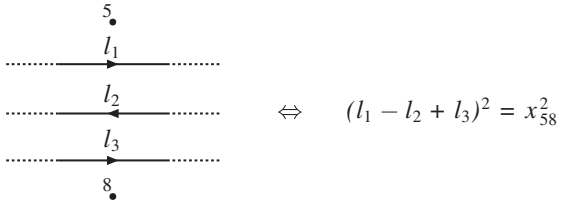

FIG. 6. The notation used in this section for listing out the pseudoconformal integrals contributing at five loops. The momentum flow through a line connecting points 5 and 8 gives the momentum invariant x_{58}^2.

$(L + 1)$-particle cut used in the construction. Since our construction was only a bookkeeping device for finding pseudoconformal integrals, at the end there is no on shell restriction on the l_i.

In the next section we apply this procedure to construct a basis of all pseudoconformal integrals appearing in the five-loop planar MSYM amplitudes.

V. FIVE-LOOP PLANAR PSEUDOCONFORMAL INTEGRALS

A. Five-loop pseudoconformal integral basis

Following the procedure described in the previous section we find a total of 59 independent pseudoconformal integrals potentially present in the five-loop four-point planar amplitude (not counting those related by permutations of external legs). They are shown in Figs. 7–10. The "parent" integrals, shown in Fig. 7, have only cubic vertices. The remaining integrals have both cubic and quartic vertices. They may be obtained by omitting propagators and modifying numerator factors present in the parent integrals, As we shall show in the following section using unitarity cuts, the integrals in Figs. 7 and 8 appear in the amplitude (2.2) with relative coefficients of ± 1, which we have absorbed into the definitions of the numerator factors in the figures. The remaining ones shown in Figs. 9 and 10 do not appear at all. We do not have an explanation for the remarkable simplicity of the coefficients of the integrals, but presumably it is tied to the superconformal invariance of the theory.

We draw the diagrams in momentum space, but also include the relevant x_i for tracking numerator factors. The numerators are written out as Mandelstam variables $s = (k_1 + k_2)^2$ and $t = (k_2 + k_3)^2$ or as dual invariants, x_{ij}^2. As discussed in Sec. III a dual invariant x_{ij}^2 is equal to K^2

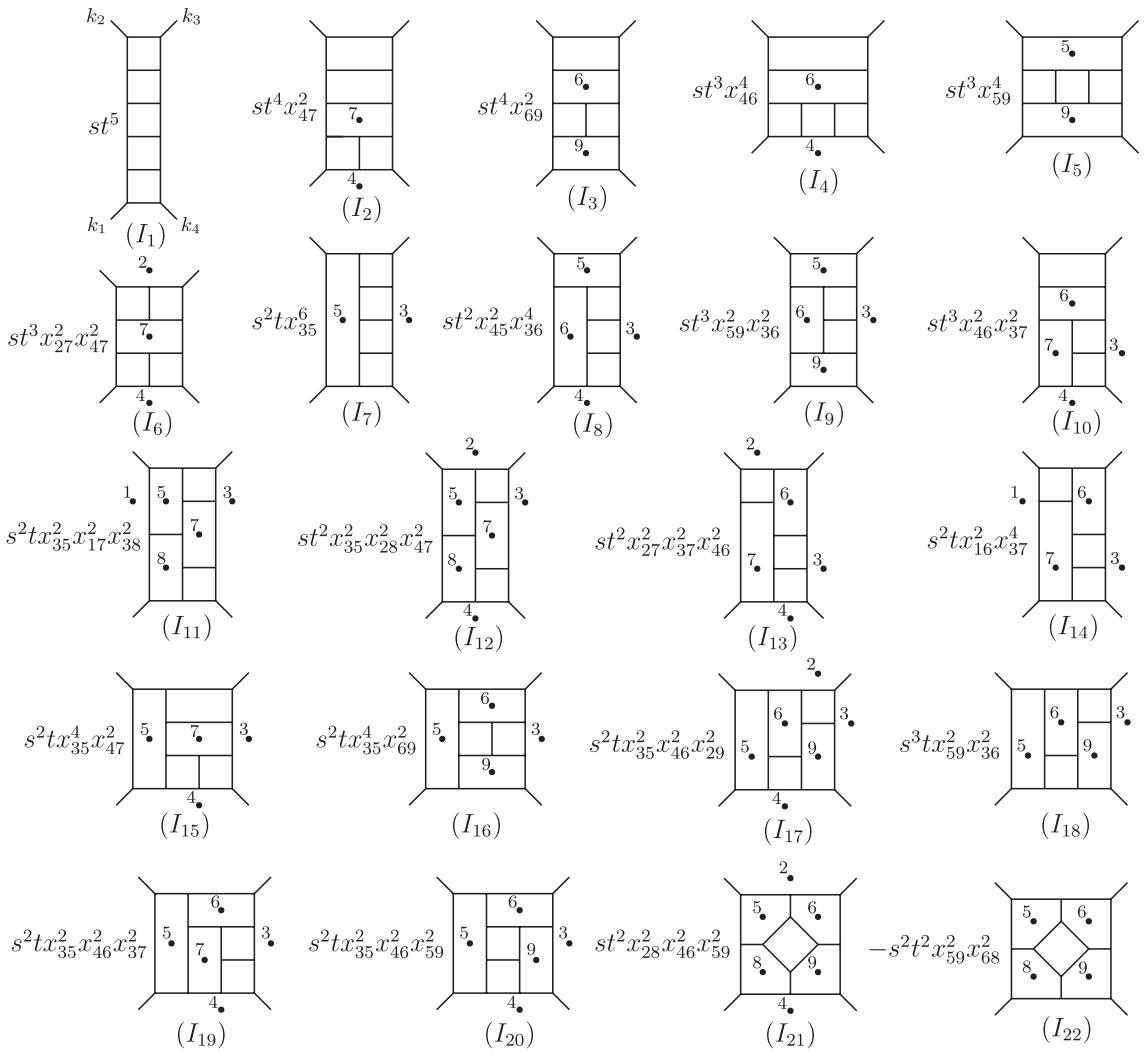

FIG. 7. All pseudoconformal integrals with only cubic vertices that contribute to the amplitude. The relative signs are determined from unitarity cuts in Secs. VII and VIII.

where K is the total momentum flowing through a line spanned between points i and j. For example, in Fig. 6, $K^2 = (l_1 - l_2 + l_3)^2 = x_{58}^2$.

Some of the integrals have identical sets of propagators but differing numerator factors. These *sibling* integrals would be identical were one to omit the numerators. Examples are I_{11} and I_{12} or I_{21} and I_{22} in Fig. 7. The numerator factors often have different symmetries than the propagators in any given integral. The different numerator factors in sibling integrals will also typically have different symmetries. For example, integral I_{22} is completely symmetric under a cyclic permutation of its arguments, $\{1, 2, 3, 4\} \to \{2, 3, 4, 1\}$ (corresponding to a $\pi/2$ rotation of the diagram in Fig. 7) and under flips, $\{1, 2, 3, 4\} \leftrightarrow \{4, 3, 2, 1\}$ (corresponding to reflection of the diagram). Its sibling I_{21}, in contrast, has only one symmetry, $\{1, 2, 3, 4\} \to \{3, 4, 1, 2\}$ (corresponding to a rotation of the diagram by π radians). Accordingly, I_{22} appears only once in the amplitude, but I_{21} appears four times. This makes it inconvenient to combine them into a single integral.

All planar five-loop pseudoconformal integrals with the exception of I_{59} have at most four-point vertices. (I_{59} has quintic vertices where the external legs attach. Internal quintic vertices do not occur in conformal integrals until seven loops.)

B. Five-loop four-point amplitude

In Secs. VII and VIII, we evaluate a sufficient number of cuts in order to determine the numerical prefactors of each pseudoconformal integral as it appears in the amplitude (2.2). We find that the complete five-loop four-point MSYM planar amplitude is

$$M_4^{(5)}(1,2,3,4) = -\frac{1}{32}[(I_1 + 2I_2 + 2I_3 + 2I_4 + I_5 + I_6 + 2I_7 + 4I_8 + 2I_9 + 4I_{10} + 2I_{11} + 4I_{12} + 4I_{13} + 4I_{14} + 4I_{15} + 2I_{16} + 4I_{17} + 4I_{18} + 4I_{19} + 4I_{20} + 2I_{21} + 2I_{23} + 4I_{24} + 4I_{25} + 4I_{26} + 2I_{27} + 4I_{28} + 4I_{29} + 4I_{30} + 2I_{31} + I_{32} + 4I_{33} + 2I_{34} + \{s \leftrightarrow t\}) + I_{22}], \tag{5.1}$$

where the integrals are shown in Figs. 7 and 8, and $M_4^{(5)}$ is defined in Eq. (2.2). There are a total of 193 integrals in the sum. As the integrals depend only on the kinematic invariants s and t, instead of having leg labels, each integral can appear only as $I_j(s, t)$ or as $I_j(t, s)$. In Eq. (5.1), we have suppressed the arguments "(s, t)" and combined identical terms, leaving a

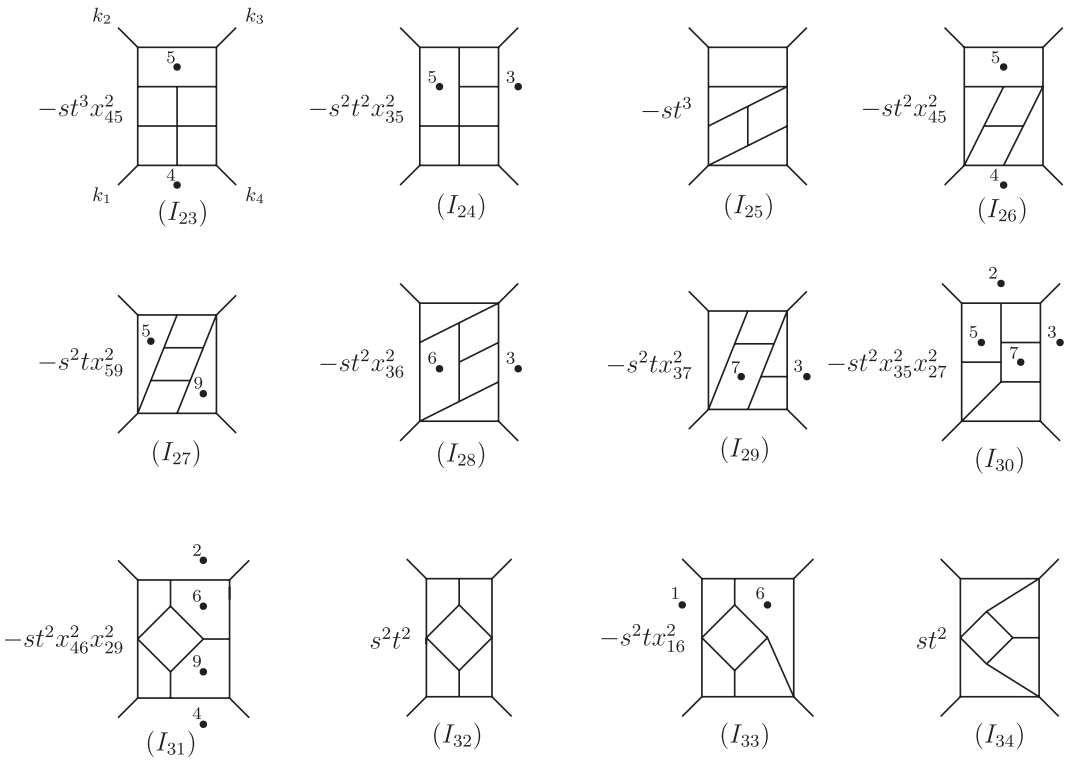

FIG. 8. All pseudoconformal integrals with cubic and quartic vertices that contribute to the amplitude. The relative signs are determined from unitarity cuts in Secs. VII and VIII.

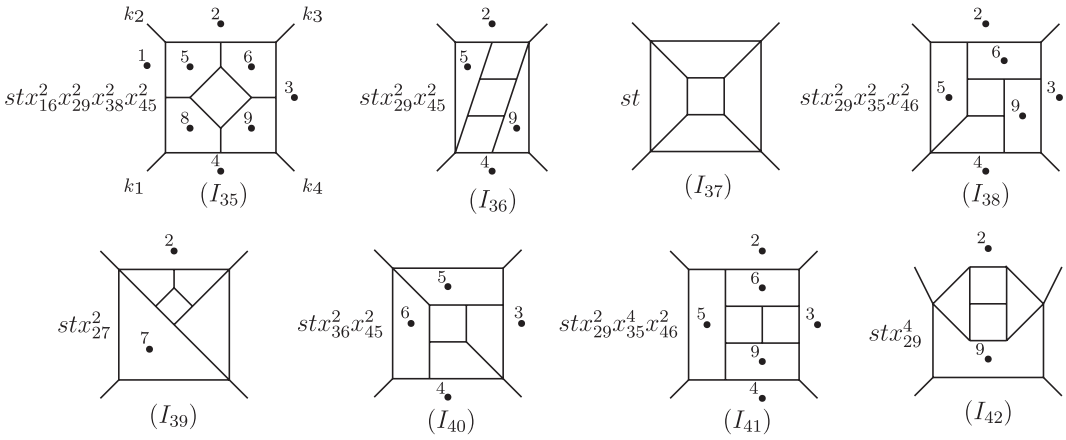

FIG. 9. A class of pseudoconformal integrals which do not contribute to the amplitude, as determined from the unitarity cuts. All these have exactly one factor of st.

symmetry factor in front. The relative signs between integrals, determined from the unitarity cuts in Secs. VII and VIII, have been incorporated in the numerator factors in Figs. 7 and 8, though we have chosen to leave an overall sign outside the integrals. The normalization factor of $1/32$ follows the conventions of Refs. [4,10] and accounts for the factor of 2^L in Eq. (2.1). The integrals in Eq. (5.1) are therefore normalized as

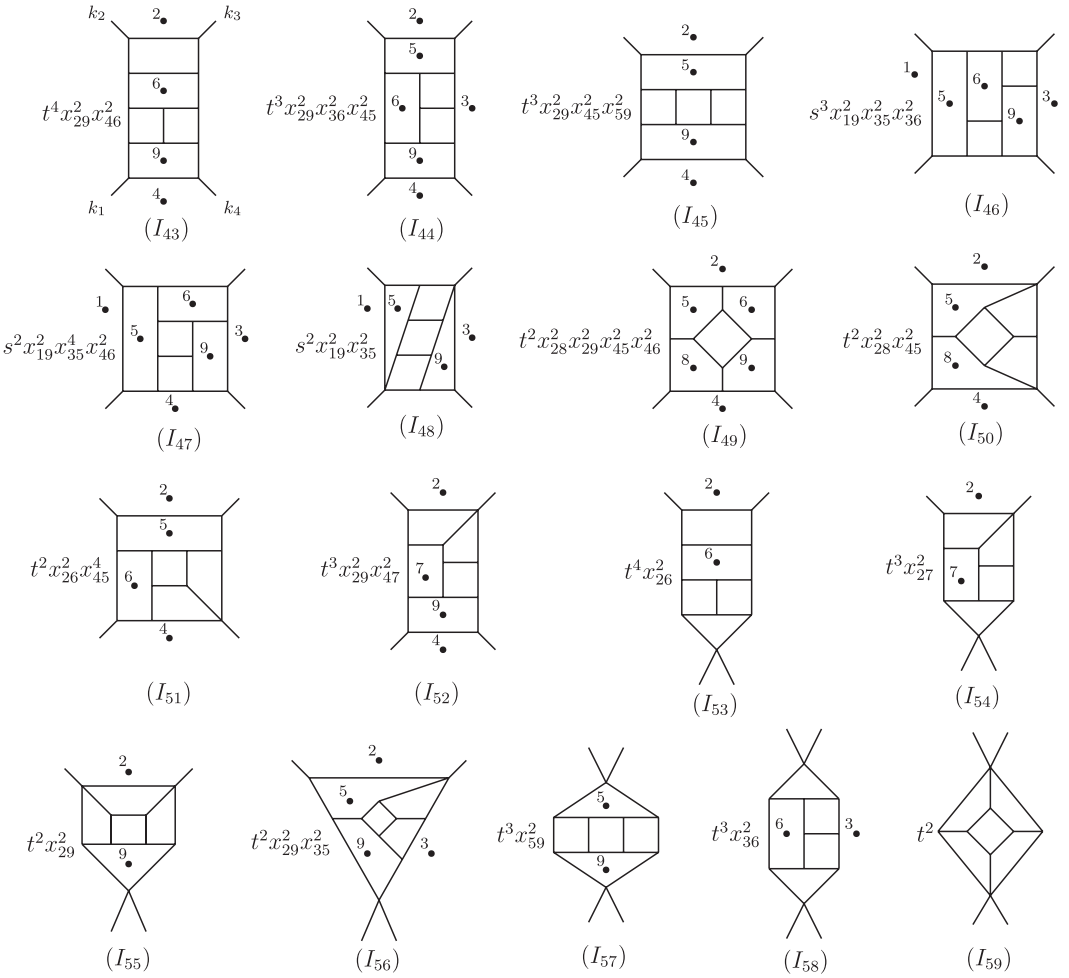

FIG. 10. The non-st class of pseudoconformal integrals. They do not contribute to the amplitude.

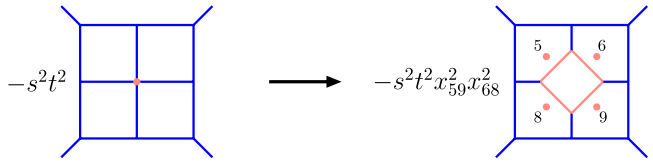

FIG. 11 (color online). The "substitution rule" is a rule for replacing any four-point vertex with terms in a four-point amplitude. Here integral I_{22} is obtained by substituting the pseudoconformal box integral appearing in the one-loop amplitude into the central vertex of the four-loop window diagram.

$$(-ie^{\epsilon\gamma}\pi^{-D/2})^5 \int \left(\prod_{i=1}^{5} d^D l_i\right) \frac{N}{\prod_j p_j^2}, \tag{5.2}$$

where the l_i are five independent loop momenta, N is the numerator factor appearing as the coefficient of the diagrams given in Figs. 7–10, and the p_j^2 correspond to the propagators of the diagrams.

To understand the relative signs of the diagrams we classify terms into those derived from the rung rule and the rest. Any diagram generated by the rung rule in Fig. 2 simply inherits the sign of the lower loop diagram from which it was derived. This gives the correct numerator factor, including the sign, for all contributing integrals containing only cubic vertices, except for I_{22}—the only diagram in Fig. 7 having a non-rung-rule numerator. Integrals with quartic vertices, such as I_{24}, I_{27}, I_{28}, and I_{29}, are given by the rung rule applied to known [10] four-loop diagrams. Using two-particle cuts, other examples of integrals whose prefactors are easy to understand are I_{23}, I_{25}, I_{26}, I_{41}, and I_{42}. The latter two have vanishing coefficient because their four-loop parent diagrams also have vanishing coefficients. Integral I_{33} can be understood in terms of a rung inserted between an external leg and an internal line.

Another class of prefactors and signs can be understood from a "substitution rule." Consider diagram I_{22} in Fig. 7. As shown in Fig. 11, this diagram inherits its prefactor and sign by replacing the four-point vertex by a one-loop box integral. (The one-loop box enters with a relative plus sign.) The numerator factor $x_{59}^2x_{68}^2$ of the substituted box is simply the factor needed to make the box conformal. The negative sign is inherited from the sign of the four-loop diagram. Also other signs can be understood from this substitution rule. For example, the sign on I_{30} and the zero coefficient on I_{53} follow from similar substitutions on four loop conformal diagrams. This rule can more generally be understood as a substitution of the normalized four-point function into a four-point vertex, which can be obtained using generalized cuts.

With the rung rule, two-particle cuts, and substitution rule we may understand the signs of all diagrams that appear in the amplitude, except for I_{31}, I_{32}, and I_{34}. As of yet we have not found a rule giving the sign of these diagrams, other than resorting to computations of cuts.

At four loops [10], integrals not containing at least one factor of s and also one factor of t are absent from the amplitude. This is again true at five loops. Factorization arguments using complex momenta can give a suggestive explanation of this property. As we already noted, supersymmetry identities ensure that after dividing by the tree amplitude, the nonvanishing MSYM four-point loop amplitudes are identical for all external helicity and particle configurations. Consider then the helicity configuration $1^-, 2^+, 3^-, 4^+$, with all external legs gluons. The tree amplitude

$$A_4^{\text{tree}}(1^-, 2^+, 3^-, 4^+) = i\frac{\langle 1\,3\rangle^4}{\langle 1\,2\rangle\langle 2\,3\rangle\langle 3\,4\rangle\langle 4\,1\rangle} = -i\frac{\langle 1\,3\rangle^2[2\,4]^2}{st} \tag{5.3}$$

factorizes in both the s and t channels into products of three-point vertices. The absence of compensating factors of s and t would imply factorization into one-particle irreducible loop three vertices. Such vertices have not appeared in the factorization of any previous MSYM amplitude, and so it is not surprising that the offending integrals, shown in Fig. 10, do not contribute here either.

We may understand the remaining vanishing coefficients using the known harmonic-superspace power counting of MSYM [47]. It is compatible in $D = 4$ with six powers of loop momenta canceling from integral numerators. The missing engineering dimensions of the amplitude are then supplied by external momenta, requiring at least three powers of either s or t. This result agrees with the arguments of Refs. [24,25], which provide a bound on dimensions for which the L-loop amplitude is ultraviolet finite,

$$D < \frac{6}{L} + 4, \qquad (L > 1). \tag{5.4}$$

It is natural to assume that this power counting holds independently for each integral. This rules out integrals which do not have at least three powers of s or t. This includes all of those in Fig. 9 and those with either a single power of s^2 or t^2 in Fig. 10.

C. All-loop structure

Inspecting the contributions of the integrals in the basis to the five-loop four-point amplitude reveals the following features:

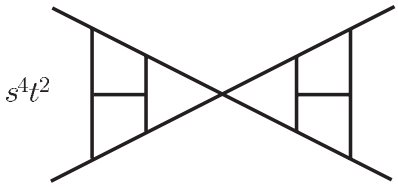

FIG. 12. A pseudoconformal integral with a vanishing coefficient in the six-loop amplitude.

(i) All pseudoconformal integrals containing a factor of s^2t or t^2s (and possibly additional powers of s or t) enter the amplitude with relative weight of $+1$ or -1.
(ii) Any pseudoconformal integral without a factor of s^2t or t^2s has a vanishing coefficient.
(iii) All integrals that could be obtained from the rung rule or from two-particle cuts inherit their weights from the lower-loop integrals used to construct them.
(iv) All contributing integrals individually satisfy the ultraviolet finiteness bound (5.4).

These observations seems to suggest that, in general, the set of pseudoconformal integrals with nonvanishing coefficients are the ones with a prefactor divisible by either s^2t or t^2s. However, at six loops a new structure appears where a pseudoconformal integral is a simple product of lower-loop integrals, as displayed in Fig. 12. We have checked that the conformal integral in Fig. 12 does not contribute to the amplitude, although its prefactor is divisible by s^2t. While this particular integral does not appear in the amplitude, its existence suggests that at higher loops there will be additional classes of pseudoconformal integrals with vanishing coefficients.

VI. GENERALIZED UNITARITY

The unitarity method [18–23,27] has proven an effective means for computing scattering amplitudes in gauge and gravity theories. So-called generalized unitarity is particularly powerful for computing amplitudes [23,27], as it allows an L-loop amplitude to be built directly from products of tree amplitudes. When combined with complex momenta [27,28,48], it allows the use of maximal cuts, in which *all* propagators in an integral are cut. (The term "generalized unitarity," corresponding to leading discontinuities of diagrams, dates back to Ref. [49].)

We begin our discussion with a brief review, including earlier applications of maximal cuts to the computation of two-loop amplitudes [29]. We record a number of observations useful for computation at higher loops. In Sec. VI A we modify the maximal-cut procedure and use it to determine the coefficients of all pseudoconformal integrals appearing in the MSYM five-loop four-point amplitudes efficiently and systematically.

A. Maximal cuts

Cut calculations can be simplified by increasing the number of cut legs. This isolates a smaller number of integrals, making it simpler to determine the values of their coefficients. This technique is especially powerful for computing one-loop MSYM amplitudes, because only box integrals can appear [18]. As observed by Britto, Cachazo, and Feng [27], taking a quadruple cut, where all four propagators in a box integral are cut, freezes the four-dimensional loop integration. This allows its kinematic coefficient to be determined *algebraically*, with no integration (or integral reduction) required. The use of complex momenta, as suggested by twistor space theories [28], makes it possible to define massless three vertices and thereby to use quadruple cuts to determine the coefficients of all box integrals including those with massless external legs.

For three massless momenta k_a, k_b, and $k_c = -(k_a + k_b)$ one has the following consistency requirement:

$$0 = k_c^2 = (k_a + k_b)^2 = 2k_a \cdot k_b = \langle ab\rangle[ba]. \tag{6.1}$$

For real momenta in Minkowski signature, λ_{k_a} and $\tilde{\lambda}_{k_a}$ [see Eq. (2.5)] are complex conjugates of each other (up to a sign determined by incoming or outgoing nature of the corresponding particle). Hence if $\langle ab\rangle$ vanishes then $[ab]$ must also vanish. This constraint holds for all three legs a, b, c leaving no nonvanishing quantities out of which to build a three vertex. If the momenta are taken to be complex, however, the two spinors λ_{k_a} and $\tilde{\lambda}_{k_a}$ are independent. This gives two independent solutions to Eq. (6.1),

$$\langle ab\rangle = 0, \quad \text{or} \quad [ab] = 0, \tag{6.2}$$

with the other spinor product nonvanishing in each case. In the three-gluon case, there are overall two possible solutions: all λ's proportional, and hence all $\langle ij\rangle$ vanishing, or all $\tilde{\lambda}$ proportional, and hence all $[ij]$ vanishing. This means that exactly one of

$$A_3^{(-)} \equiv A_3^{\text{tree}}(a^-, b^+, c^+) = -i\frac{[bc]^3}{[ab][ca]}, \tag{6.3}$$

$$A_3^{(+)} \equiv A_3^{\text{tree}}(a^+, b^-, c^-) = i\frac{\langle bc\rangle^3}{\langle ab\rangle\langle ca\rangle} \tag{6.4}$$

does not vanish. Similar statements hold for amplitudes involving fermions or scalars: one of the two independent helicity configurations will not vanish. The nonvanishing amplitudes involving a fermion pair are

$$A_3^{\text{tree}}(a_f^-, b_f^+, c^+) = -i\frac{[bc]^2}{[ab]}, \tag{6.5}$$

$$A_3^{\text{tree}}(a_f^+, b_f^-, c^-) = -i\frac{\langle bc\rangle^2}{\langle ab\rangle}, \tag{6.6}$$

where the subscript f denotes a fermionic leg. Similarly the nonvanishing scalar amplitudes are

$$A_3^{\text{tree}}(a_s^-, b_s^+, c^+) = -i\frac{[bc][ca]}{[ab]}, \tag{6.7}$$

$$A_3^{\text{tree}}(a_s^+, b_s^-, c^-) = i\frac{\langle bc\rangle\langle ca\rangle}{\langle ab\rangle}, \tag{6.8}$$

where the subscript s denotes a scalar leg. (For complex scalars, the two helicities correspond to particle and anti-

particle.) We have chosen the signs in these amplitudes to be consistent with the supersymmetry Ward identities [41], as given in Ref. [19], and with the parity conjugation rules of Ref. [50].

The method of quadruple cuts has been generalized by Buchbinder and Cachazo [29] to two loops using hepta- and octa-cuts. Although the two-loop four-point double-box integral only has seven propagators it secretly enforces an additional, eighth constraint, yielding an octa-cut which localizes the integration completely. But as the authors of Ref. [29] point out this last cut condition is not really necessary for the evaluation of the two-loop four-point amplitude: the integrand was already independent of loop momenta after imposing the constraints from the seven on shell propagators in the hepta-cut. We will return to this point below.

Let us then focus on the constraints imposed by the delta functions corresponding to the propagators alone. In the hepta-cut construction of Ref. [29], various classes of solutions are allowed by the seven delta-function constraints arising from localizing the propagators. In the context of generalized unitarity these delta functions correspond to solving the on shell cut conditions $l_i^2 = 0$. As discussed above the solution to these conditions is always complex when three-point vertices are present. These cut conditions have a discrete set of solutions because of the twofold choice in Eq. (6.2) at each three-point vertex. Each of these solutions depends on continuous parameters, corresponding to the degrees of freedom not frozen by the cut conditions. The discrete choice coincides with the choice of three-point amplitude at each vertex $A_3^{(\pm)}$ as given in Eqs. (6.3) and (6.4) (or similar vertices for fermionic and scalar lines), which suggests a convenient way to represent the possible solutions using additional labels at the vertices of the cut diagrams. For the four-point hepta-cut two inequivalent arrangements of three-point vertices are shown in Fig. 13. External legs represent outgoing external momenta while internal lines represent cut propagators and thus on shell loop momenta. The signs inside the blobs in the diagrams indicate the corresponding choice for the three-point vertex, and implicitly, that the spinors of the opposite helicity are proportional. A "⊖" vertex will have all λ spinors proportional to each other, so that the vertex is built out of $\tilde{\lambda}$ spinors of the attached legs, while the roles of the two kinds of spinors are interchanged for a "⊕" vertex. We can sum over all possible solutions to obtain the multiply cut integrand, as was done in Ref. [29]. For the sevenfold cut of the double-box diagram, there are six distinct solutions of the two types shown in Fig. 13.

Once we choose external helicities, as in Fig. 14, the blobs then dictate the possible assignments of helicities for internal lines. The rules for finding the complete set of kinematic solutions associated with a given assignment of plus and minus labels to a diagram are as follows:

(i) A ⊖ label means the three λ spinors corresponding to the lines attached to the blob are proportional to each other. Similarly, a ⊕ label denotes having the three $\tilde{\lambda}$ spinors proportional to each other.

(ii) If one of the lines attached to a vertex is an external line k_i then the spinors are proportional to an external spinor, either λ_{k_i} or $\tilde{\lambda}_{k_i}$.

(iii) If a ⊕ vertex is directly connected to another ⊕ vertex then all $\tilde{\lambda}$'s of the lines attached to both vertices are proportional to each other. A similar statement holds for the λ's of two connected ⊖ vertices.

(iv) If there is a chain of vertices of the same sign connecting any two external lines then the diagram vanishes, because one cannot solve the on shell and momentum conservation constraints for the diagram. A solution would require that two *external* spinors of the same type are proportional to each other; this cannot be true in general, because they are independent.

Applying these rules to the four-point double box does indeed give the six allowed solutions of the two types shown in Fig. 13. The remaining solutions are related to the depicted ones by flip symmetries. The complete set of solutions to the cut constraints is solely determined by the topology of a given diagram. Each solution determines a pattern of ⊕ and ⊖ vertices in the diagram. For each

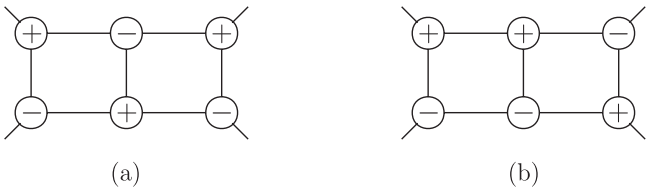

FIG. 13. A pictorial representation of two kinematic solutions to the four-point hepta-cut equations. The diagrams representing the remaining four solutions can be obtained by reflection symmetries of these. A "⊕" vertex represents a three-point tree amplitude involving only λ spinors and a "⊖" vertex represents an amplitude involving only $\tilde{\lambda}$ spinors. All lines are cut and carry on shell momenta.

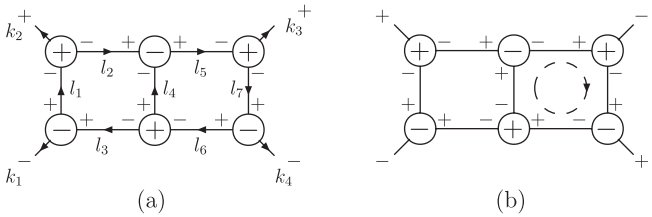

FIG. 14. A singlet hepta-cut (a) and one of the two helicity configurations (b) in the simplest nonsinglet cut. The latter allows gluons, fermions, and scalars to propagate in the loop indicated by a dashed circle. The other configuration is obtained by flipping all the helicity signs of the legs in this loop. All lines in this figure are cut and carry on shell momenta. The arrows in (a) refer to the direction of momentum flow.

solution to the cut constraints, one of the two types of three-point amplitudes vanishes at each vertex. This pattern (along with the topology) will in general restrict the helicity assignments along internal lines, and may also restrict the particle types allowed in different internal lines.

The strongest constraint that can arise in a kinematic solution is the restriction to a single allowed helicity configuration for the internal lines. We will refer to this configuration as a "singlet." In this case only gluons can propagate inside the diagram, as in Fig. 14(a). Fermions or scalars are not allowed because the only potentially nonvanishing vertices are of the wrong type and vanish for the given solution. The second-strongest constraint allows two helicity configurations. In such configurations the particle content is purely gluonic except for one loop in which any particle type can propagate, as shown in Fig. 14(b). (A fermionic loop always allows two helicity assignments, corresponding to interchanging fermion and antifermion, and the same is true for complex scalar loops.)

Solving for the spinors in any diagram is then straightforward. Consider the singlet case, Fig. 14(a). The on shell conditions together with momentum conservation at each vertex give a set of equations that must be satisfied,

$$\begin{aligned}
&\lambda_{k_1} \propto \lambda_{l_3} \propto \lambda_{l_1}, && \lambda_{k_1}\tilde{\lambda}_{k_1} = \lambda_{l_3}\tilde{\lambda}_{l_3} - \lambda_{l_1}\tilde{\lambda}_{l_1},\\
&\tilde{\lambda}_{k_2} \propto \tilde{\lambda}_{l_1} \propto \tilde{\lambda}_{l_2}, && \lambda_{k_2}\tilde{\lambda}_{k_2} = \lambda_{l_1}\tilde{\lambda}_{l_1} - \lambda_{l_2}\tilde{\lambda}_{l_2},\\
&\tilde{\lambda}_{k_3} \propto \tilde{\lambda}_{l_5} \propto \tilde{\lambda}_{l_7}, && \lambda_{k_3}\tilde{\lambda}_{k_3} = \lambda_{l_5}\tilde{\lambda}_{l_5} - \lambda_{l_7}\tilde{\lambda}_{l_7},\\
&\lambda_{k_4} \propto \lambda_{l_7} \propto \lambda_{l_6}, && \lambda_{k_4}\tilde{\lambda}_{k_4} = \lambda_{l_7}\tilde{\lambda}_{l_7} - \lambda_{l_6}\tilde{\lambda}_{l_6},\\
&\tilde{\lambda}_{l_4} \propto \tilde{\lambda}_{l_6} \propto \tilde{\lambda}_{l_3}, && \lambda_{l_4}\tilde{\lambda}_{l_4} = \lambda_{l_6}\tilde{\lambda}_{l_6} - \lambda_{l_3}\tilde{\lambda}_{l_3},\\
&\lambda_{l_4} \propto \lambda_{l_5} \propto \lambda_{l_2}, && \lambda_{l_4}\tilde{\lambda}_{l_4} = \lambda_{l_5}\tilde{\lambda}_{l_5} - \lambda_{l_2}\tilde{\lambda}_{l_2}
\end{aligned} \tag{6.9}$$

The solution to these equations is

$$\begin{aligned}
&\lambda_{l_1} = \lambda_{k_1}, && \tilde{\lambda}_{l_1} = \xi\tilde{\lambda}_{k_2},\\
&\lambda_{l_2} = \xi\lambda_{k_1} - \lambda_{k_2}, && \tilde{\lambda}_{l_2} = \tilde{\lambda}_{k_2},\\
&\lambda_{l_3} = \lambda_{k_1} && \tilde{\lambda}_{l_3} = \xi\tilde{\lambda}_{k_2} + \tilde{\lambda}_{k_1}\\
&\lambda_{l_4} = \lambda_{l_2} && \tilde{\lambda}_{l_4} = \tilde{\lambda}_{l_3}\frac{[23]}{[3l_3]}\\
&\lambda_{l_5} = \lambda_{l_2} && \tilde{\lambda}_{l_5} = \tilde{\lambda}_{k_2} + \tilde{\lambda}_{l_4}\\
&\lambda_{l_6} = \lambda_{k_1} + \lambda_{l_2}\frac{[23]}{[3l_3]} && \tilde{\lambda}_{l_6} = \tilde{\lambda}_{l_3}\\
&\lambda_{l_7} = \lambda_{k_4} && \tilde{\lambda}_{l_7} = \tilde{\lambda}_{k_3}\frac{\langle 3l_2\rangle}{\langle l_2 4\rangle},
\end{aligned} \tag{6.10}$$

where ξ is an arbitrary parameter, corresponding to the remaining degree of freedom in the integration not frozen by the hepta-cut. Since a bispinor $p^{a\dot{a}} = \lambda^a\tilde{\lambda}^{\dot{a}}$ is invariant under a rescaling of the spinors, $(\lambda^a, \tilde{\lambda}^{\dot{a}}) \to (\beta\lambda^a, \beta^{-1}\tilde{\lambda}^{\dot{a}})$, the above solution can be written in many other forms. In addition, there is a choice as to where to include the remaining degree of freedom. While individual three-point amplitudes $A_3^{(\pm)}$ are not invariant under this transformation, the product of amplitudes forming the cut is invariant.

B. Solving for integral coefficients using maximal cuts

We now consider how to solve for the coefficient of an integral using the maximal cuts. At two loops, there is only a single conformal integral, the double box. It can appear, of course, in both s- and t-channel configurations, but the hepta-cut shown in Figs. 13 and 14 selects only the s-channel double box. Our candidate expression for the amplitude is then

$$A^{(2)}(1,2,3,4) = cA^{\text{tree}}(1,2,3,4)I^{(2)}(s,t), \tag{6.11}$$

where $I^{(2)}(s,t)$ is the pseudoconformal two-loop double-box integral in Eq. (3.1) and c is a coefficient that we need to solve for. This integral contains a factor of s^2t in the numerator, which as we shall see is necessary for satisfying the cut conditions.

Imposing the sevenfold cut condition, we obtain

$$\begin{aligned}
&cs^2tA^{\text{tree}}(1,2,3,4)\int d^4l_1 d^4l_7 \prod_{i=1}^{7}\delta(l_i^2)\\
&\quad = i\int d^4l_1 d^4l_7 \prod_{i=1}^{7}\delta(l_i^2)\sum_h (A_{(1)}^{\text{tree}}A_{(2)}^{\text{tree}}A_{(3)}^{\text{tree}}A_{(4)}^{\text{tree}}A_{(5)}^{\text{tree}}A_{(6)}^{\text{tree}})_h,
\end{aligned} \tag{6.12}$$

where $A_{(i)}^{\text{tree}}$ is the three-point amplitude corresponding to one of the six three vertices and the sum over helicities h runs over all possible helicity and particle configurations. (We have taken the loop integrals to be four dimensional for the purposes of our discussion here, but in any explicit evaluation of the integrals they should be continued to D dimensions to regulate the infrared singularities.)

As discussed above, the delta-function constraints are solved by a discrete set of solutions, so we obtain

$$\begin{aligned}
&cs^2tA_4^{\text{tree}}(1,2,3,4)\int d^4l_1 d^4l_7 \int \mathrm{d}\xi \sum_{j=1}^{6} J_j\delta^4(l_1 - l_1^{\text{sol}_j})\delta^4(l_7 - l_7^{\text{sol}_j})\\
&\quad = i\int d^4l_1 d^4l_7 \int \mathrm{d}\xi \sum_{j=1}^{6} J_j\delta^4(l_1 - l_1^{\text{sol}_j})\delta^4(l_7 - l_7^{\text{sol}_j})\sum_{h\in H_j}(A_{(1)}^{\text{tree}}A_{(2)}^{\text{tree}}A_{(3)}^{\text{tree}}A_{(4)}^{\text{tree}}A_{(5)}^{\text{tree}}A_{(6)}^{\text{tree}})_{j,h},
\end{aligned} \tag{6.13}$$

where j runs over the different kinematic solutions, $l_1^{\mathrm{sol}_j}$ and $l_7^{\mathrm{sol}_j}$ are the values of the independent loop momenta expressed in terms of the external momenta, and the remaining degree of freedom is ξ. For each discrete solution j, only a subset of helicity and particle configurations denoted by H_j gives a nonvanishing contribution. The Jacobian from the change of variables is J_j.

Buchbinder and Cachazo [29] noted that the integrand is constant after imposing the seven cut conditions arising directly from cutting propagators, without need to impose the eighth cut condition. Another curiosity they noted is that all six discrete kinematic solutions for the hepta-cut give the same answer for the amplitude. This was true for kinematic solutions that permitted only gluons in the two loops as well as for those which also permitted fermions and scalars. This simplicity is related to the absence of terms which integrate to zero upon performing the loop integral.[4]

We will exploit this observation, and assume its generalization to higher loops. It allows us to match integrands, and indeed to pick individual solutions to match the left-hand and right-hand side of Eq. (6.13), determining the overall coefficient. That is, we assume that there is a single overall coefficient c to solve for in front of each integral, instead of a different contribution for each solution. This also avoids any need for integral reductions or analysis of the integrals, and translates integrands into algebraic coefficients of integrals. Our knowledge of an integral basis—given by the pseudoconformal integrals—is not essential but greatly simplifies the extraction of these coefficients. This equality of contributions from different solutions is likely special to MSYM at four points or perhaps to conformal supersymmetric gauge theories more generally. In general, there is no reason to expect solutions which allow different particle types to circulate to yield equal answers.

The assumption can be checked directly, of course, by comparing different solutions. While we have not checked it exhaustively, it does pass the large number of such comparisons that we have carried out. The use of the assumption and the maximal-cut procedure described here also leads to a determination of coefficients at three and four loops in agreement with known answers [4,10]. Furthermore, a violation would likely lead to inconsistent determinations of integral coefficients at five loops; we find no such inconsistency. We can also rely on cross-checks from nonmaximal cuts.

(The reader may be puzzled by the appearance of complex solutions in what was originally an integral over real loop momenta. This is not special to the amplitudes under consideration here. In extracting the cut by replacing propagators with delta functions, one must sum over complex solutions as well as real ones [27]. This was necessary in other circumstances such as evaluating the connected prescription for tree-level gauge-theory amplitudes [51] in twistor string theory [28]. It can also be understood by reinterpreting [52] the original integral as a fourfold contour integral in each component of the loop momentum, and replacing the propagators by products of an expression of the form $[2\pi i(l_i^\mu - l_i^{\mu,\mathrm{sol}_j})]^{-1}$ times Jacobians; Cauchy's theorem makes it act like a delta function, but allowing complex solutions. The details are not important to us here because we are only determining coefficients and not evaluating any integrals.)

Choosing one of the kinematic solutions then gives

$$cs^2tA_4^{\mathrm{tree}}(1,2,3,4) = i\sum_h (A_{(1)}^{\mathrm{tree}}A_{(2)}^{\mathrm{tree}}A_{(3)}^{\mathrm{tree}}A_{(4)}^{\mathrm{tree}}A_{(5)}^{\mathrm{tree}}A_{(6)}^{\mathrm{tree}})_h, \tag{6.14}$$

where h runs over the helicity configurations and particle content with nonvanishing contributions for the given solution.

Obviously, it is advantageous to choose the simplest solution, where the kinematics restricts us to the fewest possible particle types circulating in the loop. The best choice is a singlet where only gluons contribute. Using the kinematic solution (6.10), corresponding to the singlet solution in Fig. 14(a), we have

$$cs^2tA_4^{\mathrm{tree}}(1^-,2^+,3^+,4^-) = iA_{(1)}^{\mathrm{tree}}A_{(2)}^{\mathrm{tree}}A_{(3)}^{\mathrm{tree}}A_{(4)}^{\mathrm{tree}}A_{(5)}^{\mathrm{tree}}A_{(6)}^{\mathrm{tree}}, \tag{6.15}$$

with no sum over intermediate helicities. In the singlet case there is only one term in the helicity sum and all six three-point amplitudes are purely gluonic. Here, $A_{(j)}^{\mathrm{tree}}$ represents one of the three-gluon tree amplitudes in Eqs. (6.3) and (6.4), with the plus and minus labels on these amplitudes matching the labels of the vertices in the figure. We have confirmed that Eq. (6.15) holds for any value of the arbitrary parameter ξ (other than $\xi = 0$, where the right-hand side of Eq. (6.15) is ill defined) in the kinematic solution (6.10). This equation then determines $c = +1$, so that the pseudoconformal double-box integral in Fig. 1 appears in the two-loop amplitude with a coefficient of

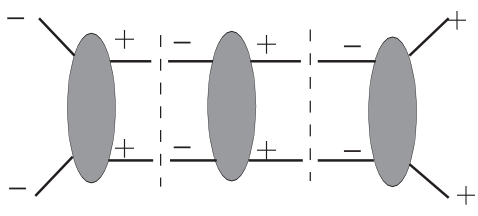

FIG. 15. A singlet iterated two-particle cut of the two-loop four-point amplitude.

[4]This property is special to four-point amplitudes and is already violated at one loop for five-point amplitudes.

$+A_4^{\text{tree}}(1^-, 2^+, 3^+, 4^-)$, in agreement with known results [24,25].

C. Generalized unitarity with real momenta at two loops

The kinematics in maximal cuts is highly constrained. It is therefore useful to have a way of checking results using less-restricted kinematics. Let us begin by considering generalized (nonmaximal) cuts which are well defined for real momenta in four dimensions.

As an example of a four-dimensional generalized cut, consider the two-loop iterated two-particle cuts shown in Fig. 15. This helicity configuration has the property that it is a singlet under supersymmetry transformations [25], the only contributions coming from gluon internal states. Hence we call it the singlet contribution. The remaining contributions, containing all other helicity and particle-type assignments, we will collectively call the "nonsinglet" contributions. These latter contributions transform into each other under supersymmetry. (The action of supersymmetry on the $\mathcal{N} = 4$ amplitudes is described in Appendix E of Ref. [25].)

The singlet configuration is especially simple to evaluate because it involves only a single particle type, similar to the singlet configurations of the maximal cuts. At higher loops, the number of different particle and helicity configurations grows rapidly. If possible, it would be simpler to use only singlet configurations to confirm our *Ansatz* for the amplitude, just as with maximal cuts. Unlike maximal cuts, however, the generalized cuts considered here do not enforce a particular choice of internal-line helicities or particle types. Nonetheless, in special cases, the singlet can be used to determine the coefficient of integrals in the amplitude.

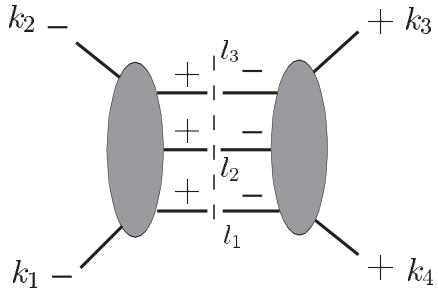

FIG. 16. A singlet contribution to the two-loop three-particle cut. Only gluons enter in the loops.

For example, in the iterated two-particle cuts at two loops shown in Fig. 15, the singlet contribution gives exactly the coefficient of the double-box integral [24]. With this external helicity configuration, this cut has no nonsinglet contribution. The nonsinglet contribution appears in the other channel and gives the identical result. In the three-particle cut, however, the singlet and nonsinglet contributions appear in the same cut and are not identical. This cut does nonetheless have simple properties that we can exploit. The singlet contribution, depicted in Fig. 16, has been previously evaluated in Refs. [24,25], with the result

$$\begin{aligned} C^{\text{singlet}} &= A_5^{\text{tree}}(1^-, 2^-, l_3^+, l_2^+, l_1^+) \times A_5^{\text{tree}}(3^+, 4^+, -l_1^-, -l_2^-, -l_3^-) \\ &= -\langle 1\,2\rangle^2[3\,4]^2 \frac{\text{tr}_+[1 l_1 4 3 l_3 2]}{(l_1 + l_2)^2(l_2 + l_3)^2(l_3 - k_3)^2(l_1 - k_4)^2(l_3 + k_2)^2(l_1 + k_1)^2}, \end{aligned} \tag{6.16}$$

where $\text{tr}_\pm[1 l_1 \cdots] = \text{tr}[(1 \pm \gamma_5)\not{l}_1 \cdots]/2$. The tree amplitudes that appear are

$$\begin{aligned} A_5^{\text{tree}}(1^-, 2^-, l_3^+, l_2^+, l_1^+) &= i \frac{\langle 1\,2\rangle^4}{\langle 1\,2\rangle\langle 2 l_3\rangle\langle l_3 l_2\rangle\langle l_2 l_1\rangle\langle l_1 1\rangle}, \\ A_5^{\text{tree}}(3^+, 4^+, -l_1^-, -l_2^-, -l_3^-) &= -i \frac{[3\,4]^4}{[3\,4][4(-l_1)][(-l_1)(-l_2)][(-l_2)(-l_3)][(-l_3)3]}. \end{aligned} \tag{6.17}$$

The nonsinglet contribution arising from the contribution of all other helicity and particle configurations crossing the cut is a bit more complicated to evaluate, and is equal to [24,25]

$$C^{\text{nonsinglet}} = -\langle 1\,2\rangle^2[3\,4]^2 \frac{\text{tr}_-[1 l_1 4 3 l_3 2]}{(l_1 + l_2)^2(l_2 + l_3)^2(l_3 - k_3)^2(l_1 - k_4)^2(l_3 + k_2)^2(l_1 + k_1)^2}. \tag{6.18}$$

The γ_5 terms in the singlet and nonsinglet appear with opposite signs. In the sum over singlet and nonsinglet contributions to the cut, the γ_5 terms therefore cancel algebraically at the level of the integrand. Alternatively, the difference between the singlet and nonsinglet contributions integrates to zero. From a practical standpoint, it is easier to compare cuts with target *Ansätze* prior to integration and to use only the singlet, so the key observation that we may use is that the non-γ_5 term of the singlet is exactly half the total contribution to the cut.

We need to extend these observations to higher loops in order for them to be useful. We have confirmed that the

same properties hold at three and four loops for any combination of two- and three-particle cuts composed only of four- and five-point tree amplitudes. (If six- or higher-point tree amplitudes are present in the cuts, non-MHV configurations with three or more negative and three or more positive helicities enter into the computation, which renders the structure of supersymmetric cancellations more elaborate and prevents us from using the singlet contribution alone to evaluate the cut.) We will assume that this observation continues to hold true at five loops. With this assumption we will be able to check (in Sec. VIII) the coefficients of a variety of pseudoconformal integrals, using only singlet cuts. This is a strong consistency check, because it relies not only on the coefficient under examination being correct, but also on the assumption remaining valid. (It seems extremely implausible that a breakdown of the assumption at five loops could be compensated by an incorrect coefficient.)

To do better we need to sum over all states crossing the cuts. Moreover, a proper treatment of the cuts requires that the cuts be evaluated using D-dimensional states and momenta [20–22]. This ensures that no contributions have been dropped, as can happen when four-dimensional momenta are used. At one loop, the improved power counting of supersymmetric theories allows one to prove a theorem that unitarity cuts with four-dimensional momenta are sufficient to determine dimensionally regulated supersymmetric amplitudes (that is, ''near'' four dimensions) completely [18,19]. (The regulator must of course maintain manifest supersymmetry; as mentioned earlier, we use the four-dimensional helicity scheme (FDH) to do so. In this scheme, the helicity algebra is always four dimensional, but the momenta are continued to $D = 4 - 2\epsilon$ dimensions.) Unfortunately, no such theorem is as yet known beyond one loop. A subtlety in deriving such a theorem arises from infrared singularities: the singularities in one loop can effectively ''probe'' the $\mathcal{O}(\epsilon)$ contributions from another loop, the product giving a surviving contribution even as $\epsilon \to 0$. When computing with D-dimensional momenta, one can no longer use the spinor helicity representation [42], which makes expressions for tree amplitudes used in the cuts more complicated. A good way to ameliorate this additional complexity is to consider instead $\mathcal{N} = 1$ in ten dimensions super-Yang-Mills dimensionally reduced to $D = 4 - 2\epsilon$ dimensions. The remaining states are completely equivalent to those of MSYM in the FDH scheme [44], except that the bookkeeping of contributions is much simpler.

At two loops all cuts of MSYM amplitudes were evaluated in D dimensions [53], providing a complete proof of the planar and nonplanar expressions for the MSYM amplitudes first obtained in Ref. [24] using four-dimensional momenta. At three loops, we have also reevaluated the planar amplitude using D-dimensional cuts. The four-loop planar amplitude has been evaluated using D-dimensional cuts, assuming that the full result (as an abstract tensor in polarization vectors and momenta) is proportional to the tree amplitude, and making the reasonable assumption that no contributions can have a triangle subintegral. (Only the terms involving polarization vectors dotted into each other, after tensor reductions, were evaluated explicitly. Also, one can rule out all bubble and some triangle subintegrals using supersymmetry along with generalized unitarity.) In Sec. VIII, we will make use of these results to provide nontrivial evidence in favor of the various assumptions we have used to obtain our *Ansatz* for the five-loop four-point planar amplitude. A complete proof would require additional D-dimensional cuts be evaluated in order to confirm the coefficient of every potential integral that might appear, including nonconformal ones.

VII. MAXIMAL-CUT TECHNIQUE FOR DETERMINING INTEGRAL COEFFICIENTS

A. Overview of maximal-cut method

In this section, we further develop the maximal-cut technique for higher loops using the observations of the previous section. This allows us to extend the two-loop maximal cuts of Buchbinder and Cachazo [29] to higher-loop orders. Unlike Buchbinder and Cachazo, we do not require the loop integration be frozen by the cut conditions. That is, we do not require the number of cut conditions to match the number of loop integrations. As discussed in the previous section, instead, we perform all evaluations of the cuts at the level of the integrand, prior to performing any loop integrations.

Moreover, we do not solve for all possible kinematic configurations satisfying the cuts. We instead focus on those solutions which allow the simplest determinations of the coefficients of the pseudoconformal integrals as they appear in the amplitude. As discussed in Sec. VI A, the simplest kinematic solutions are the singlets, to which only gluons contribute. At five loops it turns out that only four pseudoconformal integrals do not have singlet solutions. However, even in these cases one can choose kinematics which forces the fermion and scalar contributions into specific loops, again greatly simplifying the determination of the coefficients. In order to speed up the process of extracting the coefficients we solve the constraint equations numerically, although in some cases we find it useful to solve the constraints analytically.

At two, three, and four loops, where the complete results for the four-point planar amplitudes are known [4,10,24], we have confirmed that singlet maximal cuts correctly determine the coefficients of all integrals appearing in the amplitudes. This suggests that the same will be true at five loops. Again, if this were not true it would reveal itself as an inconsistency in the results. In particular, we would find that different kinematic solutions of the cut conditions would lead to inconsistent determinations of integral coefficients. We would also find inconsistencies with cuts with less restrictive kinematics.

A drawback of our maximal-cut method is its reliance on four-dimensional spinor helicity, which as mentioned in Sec. VI C might drop contributions. Nevertheless, it does provide a relatively simple and systematic means to obtain an *Ansatz* for the coefficients of integrals that appear in the amplitude.

To evaluate the coefficient of any of the five-loop integrals with only three-point vertices shown in Fig. 7, we cut all 16 propagators. Similarly, the coefficient of integrals with quartic vertices in Fig. 8 can be obtained by cutting all of the propagators present. This is of course fewer than the number of propagators present in diagrams with only cubic vertices, so some of the integrals with only cubic vertices can contribute to the cut. We must therefore subtract out all such contributions, to obtain the coefficient of a particular integral containing four-point vertices. For some solutions, the kinematics does not allow the coefficients of integrals with quartic vertices to be determined. For example, if the kinematic constraints due to three-point vertices force the spinors of two nearest neighboring legs of the four-point subamplitude to be proportional, $\lambda_i \propto \lambda_j$, the sum of momenta of these legs will be on shell, $(k_i + k_j)^2 = 0$. This can place an internal propagator of the four-point subamplitude on shell, where it diverges. This effectively selects out only those terms with this propagator present and loses the four-point contact contribution. In such cases, we determine the integral coefficient by using a different solution to the cut conditions.

B. Evaluating the five-loop integral coefficients

A maximal cut for determining the coefficient of integrals with a given set of propagators is of the form

$$C^{(5)}|_{\text{maximal}} = i^c \sum_h \left(\prod_{k=1}^{m} A^{\text{tree}}_{(k)} \right)_h, \tag{7.1}$$

where h signifies the different helicity configurations and particle types that can contribute and m is the number of tree amplitudes appearing in the cut. In this equation the cut momenta $l_1, l_2, \ldots, l_c$ are all on shell. Euler's formula relates the number of tree amplitudes that appear to the number of cut lines; at five loops $m = c - 4$. As discussed in Sec. VI A, a given kinematic solution to the cut conditions will allow only a subset of helicity configurations to contribute.

The simplest situation is when an integral has only cubic vertices, as is true for the integrals of Fig. 7. In this case one can always choose singlet kinematic solutions to the on shell conditions so that only gluons propagate in each loop. After cutting all the propagators, one obtains the numerator N subject to the cut conditions,

$$N = \left(\prod_{j=1}^{12} A^{\text{tree}}_{(j)} \right)_{\text{singlet}}, \qquad (l_1^2, l_2^2, \ldots, l_{16}^2 = 0), \tag{7.2}$$

where the tree amplitudes $A^{\text{tree}}_{(j)}$ are purely gluonic. In some cases, such as cuts isolating integrals I_1 or I_2, only a single term appears, but in others a sum of terms appear. For example, there are five contributions to the cut with propagator configuration of I_{21} and I_{22}; the integral I_{21} appears four times in the cut as well as in the amplitude, but with the numerator factor permuted, while I_{22} appears one time.

C. Examples of evaluations of integral coefficients

As a first example of the determination of the coefficient of an integral, consider the maximal cut of the "ladder" integral I_1. Here $N = ist^5 A_4^{\text{tree}}(1, 2, 3, 4)$, which is independent of the loop momenta. This coefficient was determined long ago, from iterated two-particle cuts [24]. To confirm this result using maximal cuts we solve the on shell constraints l_i^2 of all 16 cut propagators. For the external helicities $(1^-, 2^-, 3^+, 4^+)$ there are 166 distinct kinematic solutions of which 62 correspond to singlet configurations. For $(1^-, 2^+, 3^-, 4^+)$ there are 270 solutions of which 27 are singlets, and for $(1^-, 2^+, 3^+, 4^-)$ the numbers are similar: 270 solutions, with 28 singlets. We have confirmed that all these singlet solutions individually agree with the known result, providing a nontrivial check. This determines that the pseudoconformal integral I_1 enters with an overall factor of $-1/32$ in the normalized amplitude $M_4^{(5)}$ given in Eq. (5.1), after accounting for the normalization conventions of the integrals in Eq. (5.2). [The $1/32$ prefactor in Eq. (5.1) does not appear in the product of tree amplitudes making up the cut, but appears in the L-loop amplitude, due to our convention of including a factor of 2^L in Eq. (2.1).] In the integrals of Figs. 7 and 8 we have not included the overall factor of $-1/32$, but leave it as an explicit overall factor in Eq. (5.1). In the remaining part of this section, we will refer only to signs relative to I_1.

As a second example, consider I_{17} and I_{18} in Fig. 7 as well as I_{46} in Fig. 10. They have the same propagators and hence can contribute to same maximal cut. For external helicities $(1^-, 2^-, 3^+, 4^+)$ there are 335 kinematic solutions of which 62 are singlets. The helicity configuration $(1^-, 2^+, 3^-, 4^+)$ has 339 solutions and 48 singlets whereas $(1^-, 2^+, 3^+, 4^-)$ has 304 solutions and 102 singlets. Again all singlet solutions individually give results consistent with the coefficient of I_{46} vanishing and both I_{17} and I_{18} entering the amplitude with a numerical coefficient of $+1$ relative to I_1.

As a third example, consider a maximal cut of integral I_{21}. Together with integrals having the same propagators, I_{22}, I_{35}, and I_{49}, there are nine potential terms to the numerator N after symmetrization. For this cut the helicity configuration $(1^-, 2^-, 3^+, 4^+)$ has 376 solutions of which 98 are singlets and $(1^-, 2^+, 3^-, 4^+)$ has 384 solutions of which 58 are singlets. Note that helicity $(1^-, 2^+, 3^+, 4^-)$ is related to $(1^-, 2^-, 3^+, 4^+)$, by symmetry. It turns out that the singlets can never be made consistent with numerators of type I_{49}, hence its coefficient must vanish. But unfortunately, the singlet cuts do not uniquely fix the coefficients

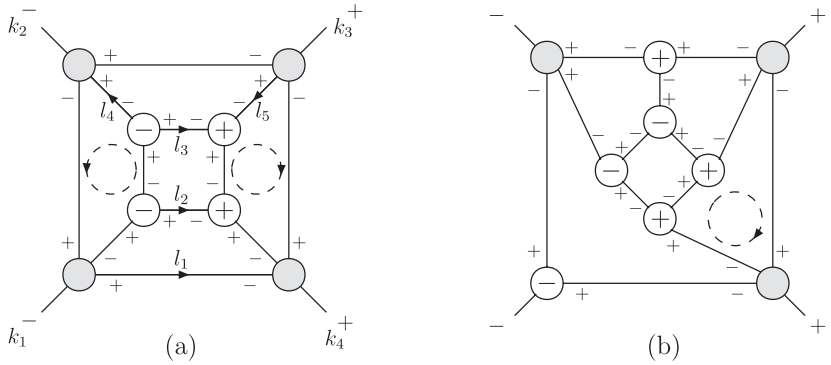

FIG. 17. (a) The simplest cut determining the coefficient of I_{37}. (b) A particularly good choice of cut for determining the coefficient of I_{39}. All lines are cut and carry on shell momenta. In all loops except those indicated by a dashed circle, only gluons propagate; the dashed circle indicates that all particle types can circulate. Other allowed helicity configurations are obtained by flipping all helicities in these loops. Grey blobs represent four-point amplitudes, which hide possible propagators inside.

of the remaining integrals. For example, if we were to assume relative numerical coefficients of ± 1, there are exactly two possibilities, one involves five terms given by symmetrizations of numerators of type I_{21} and I_{22} and the other involves two terms of type I_{35}. To resolve this situation we must instead consider cuts with fewer cut conditions imposed, to reduce the degeneracy of the kinematics.

Maximal cuts of diagrams involving noncubic vertices are only a bit more complicated. Luckily almost all cuts needed to determine the coefficients of the integrals have singlets in their solution set. Only I_{37}, I_{39}, I_{55}, and I_{59} in Figs. 9 and 10 do not have singlet solutions. For these cases we must use nonsinglet cuts, such as those in Fig. 17.

As an example of a singlet solution with a quartic vertex, consider a maximal cut of I_{32}. An expression that correctly matches the singlet maximal cut is $C_4^{(5)} = iA_4^{\text{tree}}(1, 2, 3, 4)(s^2t^2 + \cdots)$, where "$\cdots$" stands for 14 rational terms obtained from integrals I_6, I_{11}, I_{12}, I_{21}, I_{22}, and I_{31}, which also contribute to this cut. Since the coefficients of these integrals can be determined from other cuts, we simply subtract their contributions allowing us to determine the coefficient of I_{32} to be $+1$. There are now fewer cubic vertices in the cut and consequently the number of kinematic solutions also drops: The three inequivalent external helicity arrangements each have 18 solutions that are not degenerate in the two four-point blobs. However, they differ in their singlet content: Helicities $(1^-, 2^-, 3^+, 4^+)$ have four singlets, $(1^-, 2^+, 3^-, 4^+)$ have no singlets, and $(1^-, 2^+, 3^+, 4^-)$ have exactly one singlet. (When solving for the kinematics, as mentioned in Sec. VII A, we do not include solutions which are degenerate in the four-point blobs, because these do not allow us to determine I_{32}.)

As mentioned above, integrals I_{37}, I_{39}, I_{55}, and I_{59} have no singlet solutions in their maximal cuts. For I_{37} a useful choice is to force scalars and fermions to circulate in only two independent nonoverlapping loops; there is only a single kinematic solution with this property, with the helicity configuration shown in Fig. 17(a). I_{39}, I_{55}, and I_{59} all have simpler solutions with only one loop that carries fermions and scalars. For I_{39}, for example, three kinematic solutions exist with this property, one of which is displayed in Fig. 17(b).

A cut where a fermion or scalar can circulate in only one of the loops takes the form

$$C_4^{\text{5-loop}} = i^c \sum_{h\in\{+,-\}} \left\{ \left(\prod_{j=1}^{c-4} A_{(j)}^{\text{tree}} \right)_{\text{gluon}} - 4 \left(\prod_{j=1}^{c-4} A_{(j)}^{\text{tree}} \right)_{\text{fermion}} + 3 \left(\prod_{j=1}^{c-4} A_{(j)}^{\text{tree}} \right)_{\text{scalar}} \right\}, \tag{7.3}$$

where h is the helicity of the particle in the unique loop with fermions and scalars. (Helicity is conserved along this loop, which given our all-outgoing convention means that it flips going from one vertex to the next.) For the complex scalars, the two helicities correspond to particle and antiparticle. For the cut in Fig. 17(b) only four vertices involve particles other than gluons, hence five A^{tree}'s can be pulled out of the sum as a common factor. The required four-point tree amplitudes for different particles follow from the supersymmetry Ward identities [41], which are described, for example, in Appendix E of Ref. [25]. From this cut we find that I_{39} does not contribute to the amplitude. Likewise the maximal cuts of I_{55} and I_{59} show that coefficients of these integrals vanish.

For the cut in Fig. 17(a) one can arrange the kinematics so that the two loops that can carry fermions or scalars do not intersect, simplifying their evaluation. The structure is similar to Eq. (7.3), except that there are two independent sums over fermions, scalars, and gluons. We will not present it explicitly, but instead just give the kinematic solution needed for this cut,

$$
\begin{aligned}
l_1 &= p = \lambda_p \tilde{\lambda}_p, \qquad l_2 = q = \lambda_q \tilde{\lambda}_q, \\
l_3 &= -\lambda_q \tilde{\lambda}_q \frac{(p+q+k_1+k_2)^2}{\langle q^- | p + k_1 + k_2 | q^- \rangle}, \\
l_4 &= -\lambda_q \tilde{\lambda}_r \frac{(p+q+l_3+k_1)^2}{\langle q^- | p + k_1 | r^- \rangle}, \\
l_5 &= -\lambda_v \tilde{\lambda}_q \frac{(p+q+l_3-k_4)^2}{\langle v^- | p - k_4 | q^- \rangle}.
\end{aligned} \tag{7.4}
$$

Here p and q are arbitrary null vectors in four dimensions and $\tilde{\lambda}_r$ and λ_v are spinors corresponding to arbitrary null vectors r, v. The remaining seven loop momenta can be obtained by momentum conservation.

This cut is the least discriminating one needed for fixing the coefficients of the integrals in the five-loop amplitude, and hence it contains the most terms. There are 79 terms of the right conformal weight that are candidates for the left-hand side of (7.1), but of these only 28 terms contribute to the amplitude. These terms are obtained from integrals I_5, I_{16}, I_{20}, I_{21}, I_{22}, and I_{27}; the coefficient of I_{37} must thus vanish. Interestingly, this is the only maximal cut where integrals (I_{21} and I_{22}) enter twice compared to their appearance in the amplitude.

In some cases the maximal cuts cannot distinguish between different integrals, due to the degenerate nature of the kinematics. As an example, consider the maximal cut of I_{21}, I_{22}, and I_{35} described above, which has two possible numerator combinations satisfying the cut conditions. On the maximal cut of these diagrams we find

$$
(I_{21} + I_{22} - I_{35})|_{\text{cut}} = 0. \tag{7.5}
$$

The combination of I_{21} and I_{22} makes one possible numerator choice and I_{35} is another consistent choice with this maximal cut. We have checked that more than 700 kinematic solutions of this cut fail to distinguish between the possibilities. To resolve this situation we use less degenerate kinematics with fewer cut conditions imposed. The two cuts in Fig. 17, for example, resolve this ambiguity.

This type of ambiguity can even affect combinations of integrals with different sets of propagators. As a nontrivial example, the following combination of integrals vanishes in all maximal cuts we have evaluated, other than the ones in Fig. 17 and the maximal cut of I_{50}:

$$
\begin{aligned}
(I_{21} + I_{22} - I_{27} + I_{31} + I_{32} + I_{33} + I_{34} \\
- I_{35} - I_{36} + I_{38})|_{\text{cut}} = 0.
\end{aligned} \tag{7.6}
$$

This equation as well as Eq. (7.5) should be interpreted as a recipe for determining a combination of terms that can vanish in a maximal cut; if a cut picks up any integral or its permutation it should be included. (Note that the signs shown in Figs. 7 and 8 are included in the definition of these integrals.) Note that Eq. (7.5) is the same ambiguity as Eq. (7.6), but restricted to cuts of I_{21}'s topology. Other than (7.6) we have found no ambiguity that holds for all singlet solutions of a maximal cut. In any case, it can be resolved by using cuts with fewer on shell conditions. In particular, the cuts in Fig. 17 resolve the ambiguity (7.6). These cuts are only consistent with integrals I_{21}, I_{22}, I_{27}, I_{31}, I_{32}, I_{33}, and I_{34} included in the amplitude and I_{35}, I_{36}, and I_{38} excluded. It is likely that this kind of ambiguity also exists at all higher loops when using maximal cuts, but again it should be resolved by using less-restrictive cuts.

Although it is straightforward to solve analytically for any given kinematic configuration, it can get quite tedious since many of the pseudoconformal integrals have well over 100 singlet cuts each. It is therefore simpler to do so numerically. The bispinor formalism, which is automatically on shell, enables us to choose which kinematic solution to solve for numerically: Our procedure is to first assign spinors, one to each three-point vertex, with λ's assigned to each $\ominus$ vertex and $\tilde{\lambda}$'s assigned to each $\oplus$ blob. If two nearest-neighbor three-point vertices are of the $\ominus$ type, the two λ spinors of the vertices are set equal to each other. The on shell constraints force the λ spinors to be proportional to each other, but we use the rescaling freedom of the spinors, mentioned below Eq. (6.10), to set the proportionality constant to unity. Similarly, if two nearest-neighbor three-point vertices are of the $\oplus$ type, the $\tilde{\lambda}$ spinors are set equal to each other. This gives us a list of λ's and $\tilde{\lambda}$'s that uniquely specifies the solution, but their values are not yet determined. The momentum of a cut propagator between blobs of opposite sign is given by taking the tensor product of the two spinors associated with the blobs the propagator connects to. One must also allow for a complex scale factor multiplying each momentum between these blobs since it is not possible to simultaneously remove the proportionality constants in both λ and $\tilde{\lambda}$. We solve the momentum conservation constraints by numerically minimizing the sum of the squares of absolute value of all momentum conservation relations that should vanish. At the solution point this vanishes.

In some cases the numerical convergence is insufficiently fast. If necessary a given cut can always be analyzed analytically. But it is simplest to discard unstable or poorly convergent solutions because there are plenty of other solutions available. We have performed on the order of 100 singlet maximal cuts corresponding to each of the propagator configurations of the pseudoconformal basis integrals with only three-point vertices, effectively exhausting the singlets. For each integral also containing four-point vertices, we have performed on the order of 10 singlet maximal cuts, again effectively exhausting the singlets. We have also checked a handful of nonsinglet solutions, in particular, for those diagrams which have no singlet solutions. In all cases, we find that the cuts are consistent with the *Ansatz* (5.1).

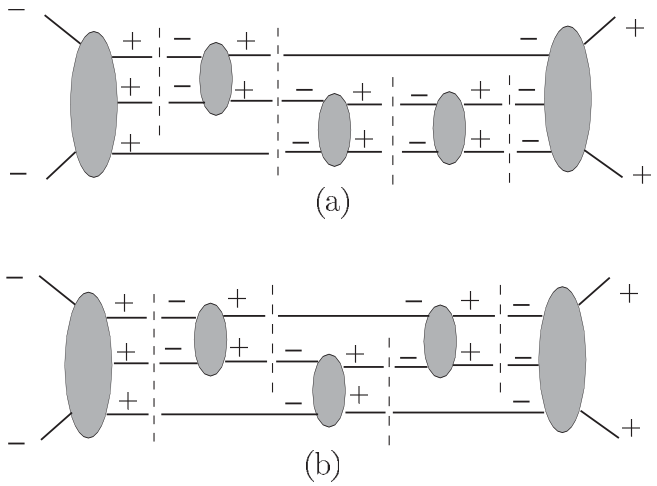

FIG. 18. The two singlet cuts containing only gluons in $D = 4$.

VIII. CROSS-CHECKS ON COEFFICIENTS FROM TWO- AND THREE-PARTICLE GENERALIZED CUTS

The kinematics used in the maximal cuts is rather restricted, so additional checks are desirable. We have evaluated two such generalized cuts in four dimensions. In D dimensions we evaluated various two-particle cuts. These cuts also provide a confirmation that no other integrals appear in the amplitudes besides the pseudoconformal ones.

A. Cuts in four dimension

The easiest four-dimensional cuts to evaluate are the singlet cuts, involving only MHV gluon tree amplitudes and a single three-particle cut, shown in Fig. 13. As described in Sec. VI, the non-γ_5 terms, obtained after dividing by the tree amplitude [see Eq. (6.16)], give precisely half the cut of the final amplitude at least through four loops. By evaluating the cuts of Fig. 18, we obtain a nontrivial check, since we find that a similar result holds at five loops.

Our evaluation confirms agreement of the non-γ_5 terms in the singlet cut of Fig. 18(a) with $1/2$ the value of the unintegrated corresponding cut of the *Ansatz* (5.1). This provides a nontrivial confirmation that we have properly determined the coefficient of integrals

$$I_3, I_8, I_9, I_{10}, I_{13}, I_{14}, I_{17}, I_{18}, \text{ and } I_{28} \tag{8.1}$$

from the maximal cuts. Similarly, we have confirmed that the non-γ_5 terms in the singlet cut 18(b) agrees with $1/2$ times the value of the corresponding cut of the *Ansatz* (5.1). This checks that the coefficients of the integrals,

$$I_2, I_3, I_6, I_9, \ldots, I_{12}, I_{17}, I_{18}, I_{25}, \text{ and } I_{30}, \tag{8.2}$$

are also correct. Moreover this also checks that integrals which have cuts of the forms in Fig. 18, but are not pseudoconformal, do not appear in the amplitude.

B. Cuts in D dimensions

A more rigorous check comes the evaluation of the D-dimensional cuts. As already mentioned, beyond one loop, no theorem has been proven that four-dimension cuts are sufficient for determining complete amplitudes in supersymmetric theories. It is therefore important to evaluate at least some cuts in D dimensions. This is especially true if we wish to apply the results away from $D = 4$.

We evaluate the D-dimensional cuts of MSYM, by interpreting it instead as ten-dimensional $\mathcal{N} = 1$ supersymmetric Yang-Mills, dimensionally reduced to D dimensions. As mentioned in Sec. VI, this way of evaluating the MSYM amplitudes has the advantage of simplifying the bookkeeping on which states are present: the $\mathcal{N} = 1$ multiplet consists of only a single gluon and gluino, each of which is composed of $8N_c$ degrees of freedom. With this formulation, all states are included, using D-dimensional momenta in the cuts.

The simplest class of integrals to check in D dimensions are ones which can be constructed by iterating two-particle cuts, following the discussion of Refs. [24,25]. The two-particle sewing equation, which is valid in D dimensions, is

$$\sum_{\mathcal{N}=4 \text{ states}} A_4^{\text{tree}}(l_1, 1, 2, l_2) A_4^{\text{tree}}(-l_2, 3, 4, -l_1) = -iA_4^{\text{tree}}(1, 2, 3, 4) \frac{st}{(l_1 - k_1)^2 (l_1 + k_4)^2}. \tag{8.3}$$

Since the tree amplitude A_4^{tree} appears on the right-hand side, the same two-particle sewing algebra appears at the next loop order. The iterated two-particle cuts allow us to

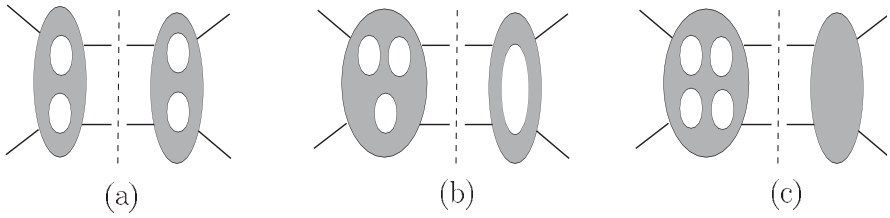

FIG. 19. The D-dimensional two-particle cut dividing the five-loop amplitude into (a) two two-loop amplitudes, (b) a one-loop and three-loop amplitude, and (c) a four-loop and a tree amplitude. All physical states are summed over in the cuts.

confirm that the coefficients of integrals,

$$I_1 \ldots I_{10}, I_{15}, I_{16}, I_{19}, I_{20}, I_{41} \ldots I_{45}, I_{47}, I_{53}, I_{57}, I_{58} \quad (8.4)$$

have all been determined correctly.

We have also checked the D-dimensional two-particle cuts which split the five-loop four-point amplitude into a product of a two two-loop amplitudes, a one-loop and three-loop amplitude and a four-loop and a tree amplitude, as depicted in Fig. 19. Using D-dimensional cuts we have evaluated the coefficients of all integrals appearing in two- and three-loop amplitudes, leaving the external legs in D dimensions. These are all proportional to the D-dimensional tree amplitude. We may likewise use the D-dimensional four-loop amplitude subject to the same assumptions made in Ref. [10], namely, the absence of certain triangle subintegrals and the appearance of the tree-level kinematic tensor as an overall coefficient. We can then apply the two-particle cut sewing equation (8.3) to confirm the coefficients of various five-loop integrals. This allows us to provide additional checks via D-dimensional unitarity that integrals

$$I_1 \ldots I_{10}, I_{15} \ldots I_{20}, I_{23}, I_{25}, I_{26}, I_{41} \ldots I_{47}, I_{51} \ldots I_{58} \quad (8.5)$$

all have the coefficients presented in Sec. VII.

To have a complete proof that the *Ansatz* (5.1) is complete, one would need to confirm from D-dimensional unitarity that these remaining integrals enter with the coefficients determined in Sec. VII and that there are no other (nonconformal) integrals present. We leave this for future work.

In general, it is rather surprising that four-dimensional unitarity cuts are sufficient to determine the amplitudes in all dimensions. The maximally supersymmetric theory, however, is special. Our D-dimensional study here provides nontrivial evidence that at least at four points, the four-dimensional cuts suffice. This result may be understood as a direct consequence of only pseudoconformal integrals being present, with coefficients independent of the number of dimensions.

IX. CONCLUSIONS

In this paper we presented an *Ansatz* for the five-loop four-point planar amplitude of maximally supersymmetric Yang-Mills amplitudes in terms of a set of pseudoconformal integrals [10,30]. We introduced a method based on cutting the maximal number of propagators [27,29] in each integral, to determine very efficiently the coefficients of the integrals as they appear in the amplitude. We then used generalized unitarity [23] with less restrictive cuts, both in four and D dimensions, to verify the correctness of the expressions determined in this way.

Our *Ansatz* for the planar five-loop four-point amplitude relies on a basis of pseudoconformal integrals, and assumes that the amplitude can be expressed entirely in terms

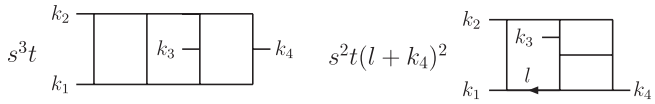

FIG. 20. Nonplanar examples of three-loop integrals confirmed by cutting all the propagators. These agree with the results of Ref. [25].

of such integrals. These integrals are the dimensionally regulated counterparts of off shell conformal integrals [10,30], limited to those which have logarithmically divergent on shell limits. This assumption has been tested and confirmed by explicit calculation through four loops. The assumption provides a compact basis of (plausibly independent) integrals, and reduces the problem of computing the amplitude to that of determining the coefficients of each integral. We have provided strong evidence that this continues to hold through at least five loops, through the evaluation of a large variety of generalized unitarity cuts, including ones evaluated in D dimensions. The computation of additional cuts in D dimensions would make it possible to prove that our expression is indeed complete. Alternatively, we may wonder whether it is possible to link to the position space conformal invariance of the theory to the absence of nonpseudoconformal integrals. An important cross-check would come from showing that the infrared singularities of the amplitude have the predicted form [4,43].

The set of integrals that appears in the expression for an L-loop MSYM amplitude is a subset of all pseudoconformal integrals. It is interesting that the integrals which do appear, do so with coefficients ± 1. We presented heuristic rules which give a partial understanding of the signs of these coefficients. It would of course be very useful to have a complete set of heuristic rules for predicting all signs and zeroes to arbitrary loop order.

This maximal form of generalized unitarity we employed should also prove useful for determining nonplanar contributions. For example, the nonplanar contributions to the subleading-color three-loop amplitude shown in Fig. 20 are easily determined from maximal cuts. These contributions are in agreement with known results [25,35]. [Note that with the cut conditions imposed $(l + k_4)^2$ and $2l \cdot k_4$ are indistinguishable in the second integral of Fig. 20, so other cuts are necessary to determine the proper factor.]

Our determination of coefficients also relied on special properties of the four-point amplitude. How can one compute amplitudes with a larger number of external legs? While some extension to the techniques presented in the present paper will certainly be necessary, they provide a very good starting point. In the planar two-loop five-point amplitude [9,26], for example, terms with even parity relative to the tree amplitude also appear to be expressible purely in terms of pseudoconformal integrals. The parity-odd terms require further study.

Beyond computations of gauge-theory amplitudes, the maximal-cut method described here should also be useful in higher-loop studies of quantum gravity. Recent calculations have established [35] that the three-loop degree of divergence in four dimensions (or equivalently the critical dimension) of $\mathcal{N} = 8$ supergravity is—contrary to widely held expectations—the same as that of $\mathcal{N} = 4$ supersymmetric gauge theory. There are other indications that the supergravity theory may even be ultraviolet finite beyond three loops [33–37]. These investigations point to the need for higher-loop computations of supergravity amplitudes, in order to establish the critical dimension in which they first become ultraviolet divergent. In the approach advocated in Ref. [25], cuts of MSYM gauge-theory amplitudes can be used to construct cuts of $\mathcal{N} = 8$ supergravity amplitudes. This paper provides the required planar amplitudes at five loops. The nonplanar contributions are more difficult, but should be within reach. This task would be considerably easier if a nonplanar analog of the pseudo-conformal integrals were identified.

Our expression for the planar five-loop four-point MSYM amplitude presented in this paper has two obvious applications. The first would be the extraction of the planar five-loop cusp anomalous dimension, allowing a further check of the conjectures of Refs. [7,10]. Another application would be a five-loop check of the iterative structure of the amplitude. This would provide a rather strong check of the all-loop resummation of maximally helicity violating amplitudes proposed in Refs. [3,4], and help reinforce a link to a recent string-side computation of gluon amplitudes [12]. The latter computation, together with all-loop-order resummations, opens a fresh venue for quantitative studies of the AdS/CFT correspondence.

ACKNOWLEDGMENTS

We are grateful to Lance Dixon for many valuable discussions and suggestions. We also thank Radu Roiban, Emery Sokatchev, Marcus Spradlin, and Anastasia Volovich for helpful discussions. We thank Academic Technology Services at UCLA for computer support. This research was supported in part by the U.S. Department of Energy under Contract No. DE-FG03-91ER40662, and in part by the Swiss National Science Foundation (SNF). The figures were generated using Jaxodraw [54], based on Axodraw [55].

[1] J. M. Maldacena, Adv. Theor. Math. Phys. **2**, 231 (1998); Int. J. Theor. Phys. **38**, 1113 (1999); S. S. Gubser, I. R. Klebanov, and A. M. Polyakov, Phys. Lett. B **428**, 105 (1998); E. Witten, Adv. Theor. Math. Phys. **2**, 253 (1998); O. Aharony, S. S. Gubser, J. M. Maldacena, H. Ooguri, and Y. Oz, Phys. Rep. **323**, 183 (2000).

[2] G. 't Hooft, Nucl. Phys. **B72**, 461 (1974).

[3] C. Anastasiou, Z. Bern, L. J. Dixon, and D. A. Kosower, Phys. Rev. Lett. **91**, 251602 (2003).

[4] Z. Bern, L. J. Dixon, and V. A. Smirnov, Phys. Rev. D **72**, 085001 (2005).

[5] J. A. Minahan and K. Zarembo, J. High Energy Phys. 03 (2003) 013; N. Beisert, C. Kristjansen, and M. Staudacher, Nucl. Phys. **B664**, 131 (2003); A. V. Belitsky, A. S. Gorsky, and G. P. Korchemsky, Nucl. Phys. **B667**, 3 (2003); N. Beisert, Nucl. Phys. **B676**, 3 (2004); J. High Energy Phys. 09 (2003) 062; N. Beisert and M. Staudacher, Nucl. Phys. **B670**, 439 (2003); L. Dolan, C. R. Nappi, and E. Witten, J. High Energy Phys. 10 (2003) 017.

[6] B. Eden and M. Staudacher, J. Stat. Mech. (2006) P014.

[7] N. Beisert, B. Eden, and M. Staudacher, J. Stat. Mech. (2007) P021.

[8] F. Cachazo, M. Spradlin, and A. Volovich, J. High Energy Phys. 07 (2006) 007.

[9] F. Cachazo, M. Spradlin, and A. Volovich, Phys. Rev. D **74**, 045020 (2006); Z. Bern, M. Czakon, D. A. Kosower, R. Roiban, and V. A. Smirnov, Phys. Rev. Lett. **97**, 181601 (2006).

[10] Z. Bern, M. Czakon, L. J. Dixon, D. A. Kosower, and V. A. Smirnov, Phys. Rev. D **75**, 085010 (2007).

[11] F. Cachazo, M. Spradlin, and A. Volovich, Phys. Rev. D **75**, 105011 (2007).

[12] L. F. Alday and J. Maldacena, J. High Energy Phys. 06 (2007) 064.

[13] A. V. Kotikov, L. N. Lipatov, and V. N. Velizhanin, Phys. Lett. B **557**, 114 (2003); A. V. Kotikov, L. N. Lipatov, A. I. Onishchenko, and V. N. Velizhanin, Phys. Lett. B **595**, 521 (2004).

[14] A. V. Kotikov, L. N. Lipatov, and V. N. Velizhanin, Phys. Lett. B **557**, 114 (2003).

[15] M. K. Benna, S. Benvenuti, I. R. Klebanov, and A. Scardicchio, Phys. Rev. Lett. **98**, 131603 (2007); A. V. Kotikov and L. N. Lipatov, Nucl. Phys. **B769**, 217 (2007); J. Maldacena and I. Swanson, Phys. Rev. D **76**, 026002 (2007); L. F. Alday, G. Arutyunov, M. K. Benna, B. Eden, and I. R. Klebanov, J. High Energy Phys. 04 (2007) 082; I. Kostov, D. Serban, and D. Volin, arXiv:hep-th/0703031; M. Beccaria, G. F. De Angelis, and V. Forini, J. High Energy Phys. 04 (2007) 066.

[16] P. Y. Casteill and C. Kristjansen, arXiv:0705.0890.

[17] S. S. Gubser, I. R. Klebanov, and A. M. Polyakov, Nucl. Phys. **B636**, 99 (2002); S. Frolov and A. A. Tseytlin, J. High Energy Phys. 06 (2002) 007; M. Kruczenski, J. High Energy Phys. 12 (2002) 024; Y. Makeenko, J. High Energy

Phys. 01 (**2003**) 007.
[18] Z. Bern, L. J. Dixon, D. C. Dunbar, and D. A. Kosower, Nucl. Phys. **B425**, 217 (1994).
[19] Z. Bern, L. J. Dixon, D. C. Dunbar, and D. A. Kosower, Nucl. Phys. **B435**, 59 (1995).
[20] Z. Bern and A. G. Morgan, Nucl. Phys. **B467**, 479 (1996); A. Brandhuber, S. McNamara, B. J. Spence, and G. Travaglini, J. High Energy Phys. 10 (2005) 011; C. Anastasiou, R. Britto, B. Feng, Z. Kunszt, and P. Mastrolia, Phys. Lett. B **645**, 213 (2007); R. Britto and B. Feng, Phys. Rev. D **75**, 105006 (2007); C. Anastasiou, R. Britto, B. Feng, Z. Kunszt, and P. Mastrolia, J. High Energy Phys. 03 (2007) 111.
[21] Z. Bern, L. J. Dixon, and D. A. Kosower, Annu. Rev. Nucl. Part. Sci. **46**, 109 (1996).
[22] Z. Bern, L. J. Dixon, D. C. Dunbar, and D. A. Kosower, Phys. Lett. B **394**, 105 (1997).
[23] Z. Bern, L. J. Dixon, and D. A. Kosower, Nucl. Phys. **B513**, 3 (1998); J. High Energy Phys. 08 (2004) 012; Z. Bern, V. Del Duca, L. J. Dixon, and D. A. Kosower, Phys. Rev. D **71**, 045006 (2005).
[24] Z. Bern, J. S. Rozowsky, and B. Yan, Phys. Lett. B **401**, 273 (1997).
[25] Z. Bern, L. J. Dixon, D. C. Dunbar, M. Perelstein, and J. S. Rozowsky, Nucl. Phys. **B530**, 401 (1998).
[26] Z. Bern, J. Rozowsky, and B. Yan, arXiv:hep-ph/9706392.
[27] R. Britto, F. Cachazo, and B. Feng, Nucl. Phys. **B725**, 275 (2005).
[28] E. Witten, Commun. Math. Phys. **252**, 189 (2004).
[29] E. I. Buchbinder and F. Cachazo, J. High Energy Phys. 11 (2005) 036.
[30] J. M. Drummond, J. Henn, V. A. Smirnov, and E. Sokatchev, J. High Energy Phys. 01 (2007) 064.
[31] V. A. Smirnov, Phys. Lett. B **491**, 130 (2000); **500**, 330 (2001); **524**, 129 (2002); *Evaluating Feynman Integrals*, Springer Tracts in Modern Physics Vol. 211 (Springer, Berlin, 2004).
[32] M. Czakon, Comput. Phys. Commun. **175**, 559 (2006); C. Anastasiou and A. Daleo, J. High Energy Phys. 10 (2006) 031.
[33] Z. Bern, L. J. Dixon, M. Perelstein, and J. S. Rozowsky, Nucl. Phys. **B546**, 423 (1999); Z. Bern, N. E. J. Bjerrum-Bohr, and D. C. Dunbar, J. High Energy Phys. 05 (2005) 056; N. E. J. Bjerrum-Bohr, D. C. Dunbar, and H. Ita, Phys. Lett. B **621**, 183 (2005); N. E. J. Bjerrum-Bohr, D. C. Dunbar, H. Ita, W. B. Perkins, and K. Risager, J. High Energy Phys. 12 (2006) 072.
[34] Z. Bern, L. J. Dixon, and R. Roiban, Phys. Lett. B **644**, 265 (2007).
[35] Z. Bern, J. J. Carrasco, L. J. Dixon, H. Johansson, D. A. Kosower, and R. Roiban, Phys. Rev. Lett. **98**, 161303 (2007).
[36] Z. Bern, http://online.kitp.ucsb.edu/online/strings05/bern; Z. Bern, *The 2006 Niels Bohr Summer Institute: Frontiers in Theoretical Particle Physics* (2006), http://www.nbsi.nbi.dk/bern.ppt.
[37] G. Chalmers, arXiv:hep-th/0008162; M. B. Green, J. G. Russo, and P. Vanhove, J. High Energy Phys. 02 (2007) 099; Phys. Rev. Lett. **98**, 131602 (2007).
[38] M. B. Green, H. Ooguri, and J. H. Schwarz (private communication); arXiv:0704.0777.
[39] H. Kawai, D. C. Lewellen, and S. H. H. Tye, Nucl. Phys. **B269**, 1 (1986).
[40] M. L. Mangano and S. J. Parke, Phys. Rep. **200**, 301 (1991); L. J. Dixon, in *Proceedings of TASI '95*, edited by D. E. Soper (World Scientific, Singapore, 1996).
[41] M. T. Grisaru, H. N. Pendleton, and P. van Nieuwenhuizen, Phys. Rev. D **15**, 996 (1977); M. T. Grisaru and H. N. Pendleton, Nucl. Phys. **B124**, 81 (1977); S. J. Parke and T. R. Taylor, Phys. Lett. B **157**, 81 (1985); **174**, 465 (1986); Z. Kunszt, Nucl. Phys. **B271**, 333 (1986).
[42] F. A. Berends, R. Kleiss, P. De Causmaecker, R. Gastmans, and T. T. Wu, Phys. Lett. B **103**, 124 (1981); P. De Causmaecker, R. Gastmans, W. Troost, and T. T. Wu, Nucl. Phys. **B206**, 53 (1982); Z. Xu, D. H. Zhang, and L. Chang, Report No. TUTP-84/3-TSINGHUA; R. Kleiss and W. J. Stirling, Nucl. Phys. **B262**, 235 (1985); J. F. Gunion and Z. Kunszt, Phys. Lett. B **161**, 333 (1985); Z. Xu, D. H. Zhang, and L. Chang, Nucl. Phys. **B291**, 392 (1987).
[43] L. Magnea and G. Sterman, Phys. Rev. D **42**, 4222 (1990).
[44] Z. Bern and D. A. Kosower, Nucl. Phys. **B379**, 451 (1992); Z. Bern, A. De Freitas, L. Dixon, and H. L. Wong, Phys. Rev. D **66**, 085002 (2002); A. De Freitas and Z. Bern, J. High Energy Phys. 09 (2004) 039.
[45] W. Siegel, Phys. Lett. B **84**, 193 (1979).
[46] N. Nakanishi, *Graph Theory and Feynman Integrals* (Gordon and Breach, New York, 1971).
[47] P. S. Howe and K. S. Stelle, Phys. Lett. B **554**, 190 (2003).
[48] R. Britto, F. Cachazo, B. Feng, and E. Witten, Phys. Rev. Lett. **94**, 181602 (2005).
[49] R. J. Eden, P. V. Landshoff, D. I. Olive, and J. C. Polkinghorne, *The Analytic S Matrix* (Cambridge University Press, Cambridge, England, 1966).
[50] Z. Bern, L. J. Dixon, and D. A. Kosower, Nucl. Phys. **B437**, 259 (1995).
[51] R. Roiban, M. Spradlin, and A. Volovich, Phys. Rev. D **70**, 026009 (2004).
[52] C. Vergu, Phys. Rev. D **75**, 025028 (2007).
[53] Z. Bern, A. De Freitas, and L. J. Dixon, J. High Energy Phys. 03 (2002) 018.
[54] D. Binosi and L. Theussl, Comput. Phys. Commun. **161**, 76 (2004).
[55] J. A. M. Vermaseren, Comput. Phys. Commun. **83**, 45 (1994).